Supplementary Information

Base-triggered self-amplifying degradable polyurethanes with the ability to translate local stimulation to continuous long-range degradation

Yanhua Xu,[a] Samya Sen,[b] Qiong Wu,[a] Xujia Zhong,[a] Randy H. Ewoldt,[b] Steven C. Zimmerman[a]*

[a]Department of Chemistry, University of Illinois, Urbana, Illinois 61801, United States.
[b]Department of Mechanical Science and Engineering, University of Illinois, Urbana, Illinois 61801, United States.

*Corresponding author (sczimmer@illinois.edu)

Contents

1. Materials and Instrumentation

All reagents were purchased from Acros Organics, Fisher Scientific, Chem-Impex International, AK Scientific, TCI America, or Sigma-Aldrich and used without further purification unless otherwise noted. For the synthetic procedures, dichloromethane (DCM), pyridine, THF were taken from an SDS system. *N*-Methyl-2-pyrrolidone (NMP) was used after distillation to remove water. NMR spectra were recorded using Varian U400, UI400, U500, VXR500, UI500NB, CB500 spectrometers in the NMR laboratory, School of Chemical Science, University of Illinois. Spectra were processed by using MestRec (v4.8.1.1) or MestReNova (v. 6.1.0). NMR spectra were referenced to the residual proton solvent peak. Coupling constants are listed in Hertz (Hz). Mass spectral analyses were provided by the Mass Spectrometry Laboratory, School of Chemical Science, University of Illinois, using ESI on a Waters Micromass Q-Tof spectrometer, FD on a Waters 70-VSE spectrometer. Analytical gel permeation chromatography (GPC) experiments were performed on a hybrid system equipped with a Waters 1515 isocratic pump, a Waters 2414 refractive index detector, and a miniDAWN TREOS 3-angle laser light scattering detector (MALLS, Wyatt Technology, CA) with the detection wavelength set at 658 nm. The MALLS detector was calibrated using pure toluene and used for the determination of the absolute molecular weights. DMF containing 0.1 M LiBr was used as the mobile phase with the flow rate = 1.0 mL/min at 50 °C using a set of four Styragel columns (5 μm): two HR 2, one HR 3 and one HR 4. Absolute molecular weights of the polymers were determined based on the d_n/d_c value of each sample using the ASTRA software (version 6.1, Wyatt Technology CA) assuming 100% mass recovery. The degradation of polymer **1** with GPC was conducted in DMF on a Tosoh Ecosec HLC8320GPC at 50 °C equipped with a reference columns (7.8 mm ID × 15 cm), guard column (6.0 mm ID × 4.0 cm × 5 μm) and two analytical columns (7.8 mm ID × 30 cm × 5 μm). The reference flowrate was set to 0.5 mL/min and the analytical column flowrate set to 1.0 mL/min. Thermogravimetric analysis (TGA) was performed on a TA Instruments Q50 analyzer. Samples were heated in a platinum crucible at a rate of 5 °C/min under a nitrogen atmosphere. Differential scanning calorimetry (DSC) was measured by Discovery DSC 250 from TA Instruments. T_g was calculated by half-height midpoint method on 2nd heating cycle with a heating rate 5 °C/min. Attenuated total reflection infrared spectroscopy (ATR-IR) was performed on a Nexus 670 ThermoNicolet Fourier Transform Infrared Spectrometer. The LC-MS data were obtained on an Agilent LC/MS (XCT Plus Trap) with Agilent SB-Aq column (50 mm × 4.6 mm, 5 μm particle size) and the eluents were H_2O/CH_3CN with 0.1% formic acid. Photographs were taken using a Nikon digital camera (Canon EOS-5D Mark III Digital SLR 21. 1 MP Digital Camera). Quantification of the degradation area of the crosslinked materials versus time was conducted with the Image-Pro Plus software using the procedure in Chapter 8: Color Segmentation in the user manual: Image-Pro Plus version 5.1 for Windows. Characterization of linear viscoelastic properties was performed on a combined motor/transducer DHR-3 rotational rheometer from TA Instruments using a parallel-plate geometry with a diameter of 20 millimeters and Peltier temperature control. For rheological characterization, all gels were prepared at a nominal thickness of 1.5 mm for loading. During measurements, the gap was continuously varied to maintain a normal force of 0.5 ± 0.2 N to avoid edge fracture and maintain contact across the geometry. A low viscosity mineral oil was applied to the exposed surface of the gel to prevent evaporation. All data was plotted and fitted using OriginPro 8. Some plots were imported into Adobe Illustrator for annotation and coloring of lines and symbols.

2. Monomer and Polymer Synthesis

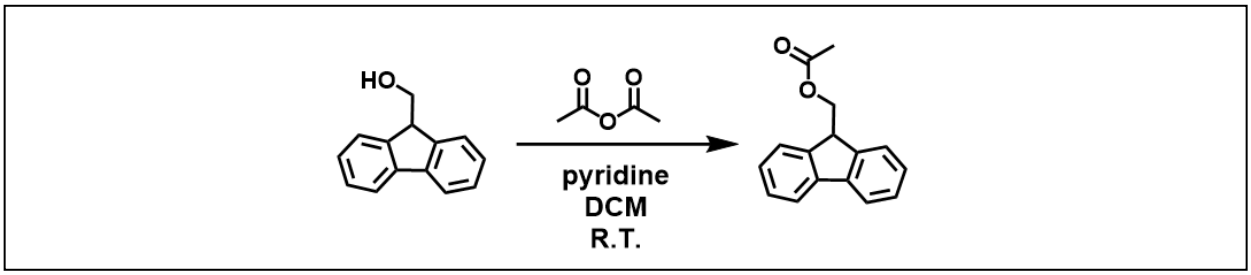

(9*H*-Fluoren-9-yl)methyl acetate. In a 500-mL round-bottom flask, 2-(9H-fluoren-9-yl)ethan-1-ol (19.6 g, 100 mmol) was dissolved in DCM (200 mL). The reaction mixture was cooled to 0 °C with an ice bath and treated with pyridine (10.5 mL, 130 mmol). Acetic anhydride (12.3 mL, 130 mmol) was added dropwise over 10 mins. The resulting solution was warmed to room temperature and stirred for 16 h. The reaction mixture was concentrated under reduced pressure and the crude residue poured into a separatory funnel containing 200 mL 1M aqueous HCl and extracted with ethyl ether (200 mL) 3 times. The combined organic layers were washed with brine (100 mL), dried over $MgSO_4$, filtered and concentrated under reduced pressure. Recrystallization from acetone afforded 19.3 g (81%) of product as a white solid. ^{1}H NMR (500 MHz, $CDCl_3$): δ 7.78 (d, *J* = 7.56, 2H), 7.61 (d, *J* = 7.49, 2H), 7.42 (t, *J* = 7.06, 2H), 7.33 (t, *J* = 7.46, 2H), 4.38 (d, *J* = 7.33, 2H), 4.22 (t, *J* = 7.31, 1H), 2.15 (s, 1H). ^{13}C NMR: (125 MHz, $CDCl_3$): δ 171.1, 143.9, 141.4, 127.9, 127.2, 125.2, 120.2, 66.6, 46.8, 21.1. High resolution ESI-MS: Calculated for $C_{16}H_{14}O_2Na^+$([M+Na]$^+$): 261.0891; obtained 261.0893.

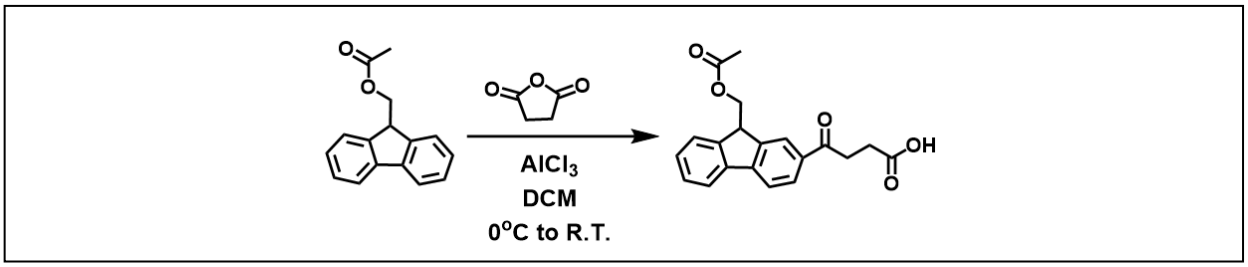

4-(9-(Acetoxymethyl)-9*H*-fluoren-2-yl)-4-oxobutanoic acid. In a 500-mL round bottom flask, succinic anhydride (8.1 g, 81 mmol) and $AlCl_3$ (32 g, 240 mmol) were dissolved in dry DCM (285 mL) at 0 °C, and (9*H*-fluoren-9-yl)methyl acetate (19.3 g, 81 mmol) dissolving in DCM (50 mL) was added dropwise over 20 min. The mixture was stirred at ambient temperature for 24 h. The reaction mixture was cooled at 0 °C with an ice bath and quenched with a 1M aqueous solution of HCl until pH = 1. The reaction mixture was extracted with ethyl acetate (200 mL) 3 times. The organic layer was washed with 1M aqueous solution of HCl (100 mL) 3 times with brine (100 mL). The solution was dried over Na_2SO_4 and concentrated by rotary evaporation. Recrystallization from acetone afforded 18.9 g (69%) of products as a white solid. ^{1}H NMR (500 MHz, $(CD_3)_2SO$) δ 12.13 (s, 1H), 8.27 (s, 1H), 8.07 (d, *J* = 7.9, 1H), 7.84 (d, *J* = 7.8, 1H), 7.63 (d, *J* = 7.5, 1H), 7.47-7.39 (m, 2H), 4.46-4.35(m, 2H), 4.28 (t, *J* = 7.1, 1H), 3.39 (t, *J* = 6.5, 2H), 2.86 (t, *J* = 6.5, 2H), 2.15 (s, 3H). ^{13}C NMR (125 MHz, $(CD_3)_2SO$): δ 198.0, 173.9, 170.3, 145.4, 145.1, 144.0, 139.6, 135.2, 128.4, 128.1, 128.0, 125.2, 124.5, 121.3, 120.2, 64.9, 46.3, 33.2, 28.0, 20.6. High resolution ESI-MS: Calculated for $C_{20}H_{19}O_5^+$([M+H]$^+$): 339.1232; obtained 339.1232.

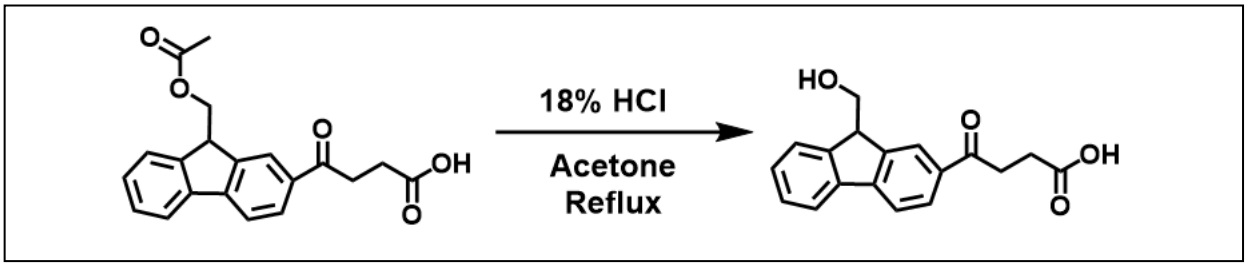

4-(9-(Hydroxymethyl)-9*H*-fluoren-2-yl)-4-oxobutanoic acid. In a 500-mL round bottom flask, 4-(9-(Acetoxymethyl)-9*H*-fluoren-2-yl)-4-oxobutanoic acid (18.9 g, 55.8 mmol) was dissolved in acetone (160 mL), and 18 wt% aqueous HCl (90 mL) was added. The mixture was refluxed for 5 h. Acetone was removed under vacuum, and solid was collected by filtration and washed with water and ethyl ether. Recrystallization from acetone afforded 12 g (72%) of the product as a white solid. ^{1}H NMR (500 MHz, $(CD_3)_2SO$): δ 8.35 (s, 1H), 8.1 (d, *J* = 7.9, 1H), 7.94-7.90 (m, 2H), 7.72 (d, *J* = 7.3, 1H), 7.46-7.39 (m, 2H), 4.14 (t, *J* = 6.7, 1 H), 4.02 (m, 1H), 3.90 (m, 1H), 3.41 (t, *J* = 6.1, 2H), 2.76 (t, *J* = 6.4, 2H). ^{13}C NMR (125 MHz, $(CD_3)_2SO$): δ 198.2, 174.0, 146.4, 145.7, 145.4, 139.6, 134.9, 128.1, 127.7, 127.5, 125.3, 124.7, 121.0, 119.9, 63.4, 50.1, 33.2, 28.0. High resolution ESI-MS: Calculated for $C_{18}H_{17}O_4^+$([M+H]$^+$): 297.1127; obtained 297.1127.

1-(9-

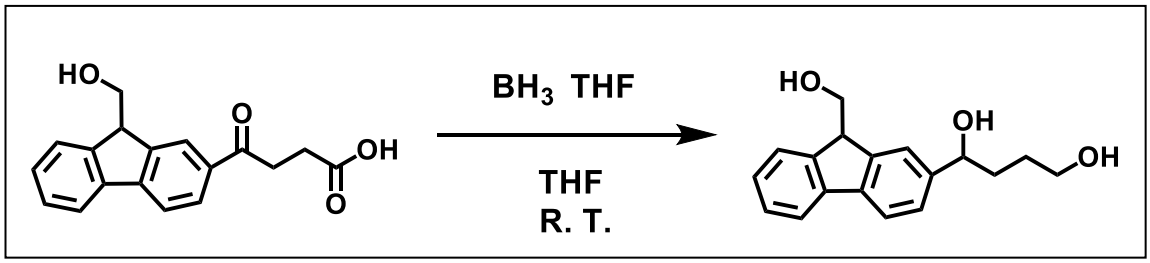

(Hydroxymethyl)-9*H*-fluoren-2-yl)butane-1,4-diol. In a 500-mL round bottom flask, 4-(9-(Hydroxymethyl)-9*H*-fluoren-2-yl)-4-oxobutanoic acid (12 g, 40.5 mmol) was dissolved in THF (60 mL). The flask was purged with argon and cooled to 0 °C with an ice bath. 1M Borane tetrahydrofuran complex (120 mL, 120 mmol) in THF solution was added dropwise over 15 min. The mixture was stirred at ambient temperature for 12 h. The reaction was cooled to 0 °C and methanol (15 mL) and H_2O (30 mL) were added to quench the reaction. The organic solution was removed under vacuum. The reaction mixture was extracted with ethyl acetate (70 mL) 3 times. The combined organic layer was washed with brine (70 mL). The solution was dried over $MgSO_4$, and concentrated using a rotary evaporator. The crude product was purified by flash chromatography eluting with 7% (v/v) MeOH in DCM and resulted in 5.1 g (44%) of product as a white powder. ^{1}H NMR (500 MHz, CD_3OD) δ 7.75 (m, 2H), 7.65 (m, 2H), 7.34-7.39 (m, 2H), 7.28 (t, *J* = 7.5, 1H), 4.71 (t, *J* = 6.7, 1H), 4.00-4.04 (m, 1H), 3.84-3.91 (m, 2H), 3.57 (t, *J* = 6.6, 2H), 1.80-1.91 (m, 2H), 1.64-1.72 (m, 1H), 1.51-1.59 (m, 1H). ^{13}C NMR: (125 MHz, CD_3OD): δ 146.4, 145.4, 142.4, 141.8, 128.4, 127.8, 126.6, 126.5, 126.1, 123.9, 123.8, 120.7, 120.5, 75.3, 65.8, 62.9, 51.6, 36.8, 30.1. High resolution ESI-MS: Calculated for $C_{18}H_{20}O_3Na^+$ ([M+Na]$^+$): 307.1310; obtained 307.1317.

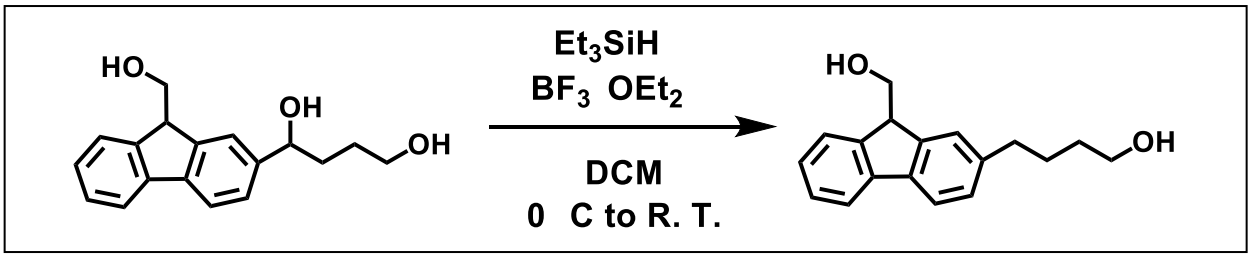

4-(9-(Hydroxymethyl)-9*H*-fluoren-2-yl)butan-1-ol. In a 50-mL round bottom flask, 1-(9-(Hydroxymethyl)-9*H*-fluoren-2-yl)butane-1,4-diol (1.52g, 5.3 mmol) and Et_3SiH (1.7 mL, 10.3 mmol) were dissolved in dry DCM (10 mL) at 0 °C with an ice bath under nitrogen, and $BF_3{\cdot}Et_2O$ (1.3 mL) was added all at once to the reaction mixture. The mixture was stirred at 0 °C for 30 min. H_2O (5 mL) was added to the mixture to quench the reaction and the mixture was extracted with DCM (10 mL) 3 times. The combined organic layer was washed with brine (10 mL). The solution was dried over $MgSO_4$, and concentrated using a rotary evaporator. The crude product was purified by flash chromatography eluting with 50% (v/v) ethyl acetate in hexane to give 0.43 g (30%) of product as a colorless liquid. ^{1}H NMR (500 MHz, $CDCl_3$): δ 7.73 (d, *J* = 7.5, 1H), 7.67 (d, *J* = 7.8, 1H), 7.58 (d, *J* = 7.4, 1H), 7.44 (s, 1H), 7.36-7.40 (m, 1H), 7.29 (t, *J* = 7.5, 1H), 7.22 (d, *J* = 7.8, 1H), 4.00-4.09 (m, 3H). 3.66 (t, *J* = 6.5, 2H), 2.73 (t, *J* = 7.6, 2H), 1.70-1.80 (m, 2H), 1.62-1.67 (m, 2H). ^{13}C NMR (125 MHz, $CDCl_3$): δ 144.8, 144.3, 141.7, 141.6, 139.4, 127.9, 127.6, 126.8, 124.9, 124.7, 120.0, 119.9, 65.3, 62.9, 50.4, 36.0, 32.4, 27.8. High resolution ESI-MS: Calculated for $C_{18}H_{21}O_2^+$([M+H]$^+$): 269.1542; obtained 269.1541.

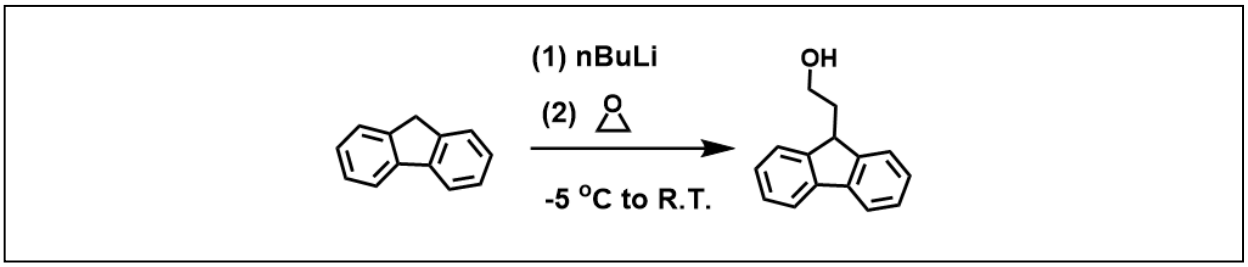

2-(9*H*-fluoren-9-yl)ethan-1-ol. The 2-(9*H*-fluoren-9-yl)ethan-1-ol was prepared using reported procedure.[1] In a 100-mL round bottom flask, 9*H*-fluorene (4.15 g, 25 mmol) was dissolved in dry THF under argon at -5 °C, and 1.6 M n-Butyllithium (15.6 mL, 25 mmol) in hexane was added dropwise over 10 min. After stirring for 10 min, 2.5-3.3M ethylene oxide (7.5 mL, 19 mmol) in THF was added rapidly, keeping the temperature below -5 °C. The reaction was slowly warmed to room temperature and was continued at room temperature for 5 h. Saturated aqueous NH_4Cl (15 mL) was added slowly to quench the reaction and the organic solution was removed using a rotary evaporator. The residue was extracted with ethyl acetate (20 mL) 3 times. The combined organic layer was washed with brine (20 mL). The solution was dried over $MgSO_4$, and concentrated using a rotary evaporator. Recrystallization from acetone afforded 3.9 g (74%) of the product as a white solid. ^{1}H NMR (500 MHz, $CDCl_3$): δ 7.77 (d, *J* = 7.5, 2H), 7.55 (d, *J* = 7.4, 2H), 7.38 (t, *J* = 7.4, 2H), 7.32 (t, *J* = 7.4, 2H), 4.14 (t, *J* = 6.0, 1H), 3.61 (t, *J* = 6.7, 2H), 2.31 (q, *J* = 6.4, 2H). ^{13}C NMR: (125 MHz, $CDCl_3$): δ 147.0, 141.1, 127.3, 127.2, 124.6, 120.1, 60.4, 44.8, 35.9. High resolution ESI-MS: Calculated for $C_{15}H_{14}O^+$([M]$^+$): 210.1045; obtained 210.1046.

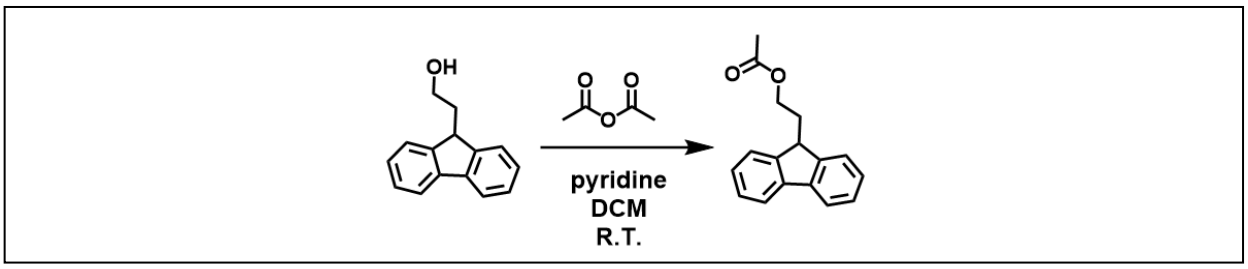

2-(9*H*-fluoren-9-yl)ethyl acetate. In a 100-mL round-bottom flask, 2-(9*H*-fluoren-9-yl)ethan-1-ol (3.9 g, 18.6 mmol) was dissolved in DCM (40 mL). The reaction mixture was cooled to 0 °C with an ice bath and treated with pyridine (1.9 mL, 24 mmol). Acetic anhydride (2.3 mL, 24 mmol) was added dropwise over 10 mins. The resulting solution was warmed to room temperature and stirred for 16 h. The reaction mixture was concentrated under reduced pressure and the crude residue poured into a separatory funnel containing 40 mL 1M aqueous HCl and extracted with ethyl ether (40 mL) 3 times. The combined organic layers were washed with brine (20 mL), dried over $MgSO_4$, filtered and concentrated under reduced pressure. Recrystallization from acetone afforded 3.5 g (75%) of product as a white solid. ^{1}H NMR (500 MHz, $CDCl_3$): δ 7.76 (d, *J* = 7.6, 2H), 7.52 (d, *J* = 7.5, 2H), 7.38 (t, *J* = 7.5, 2H), 7.32 (t, *J* = 7.4, 2H), 4.09 (t, *J* = 6.0, 1H), 4.01 (t, *J* = 6.9, 1H), 2.37 (q, *J* = 6.0, 1H), 1.90 (s, 3H). ^{13}C NMR (125 MHz, $CDCl_3$): δ 171.1, 146.4, 141.2, 127.4, 127.2, 124.5, 120.2, 61.9, 44.6, 31.7, 20.9. High resolution ESI-MS: Calculated for $C_{17}H_{17}O_2^+$([M+H]$^+$): 253.1229; obtained 253.1241.

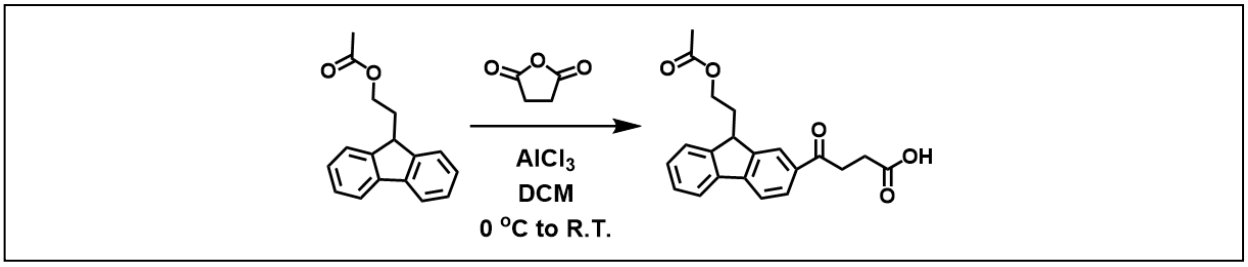

4-(9-(2-acetoxyethyl)-9*H*-fluoren-2-yl)-4-oxobutanoic acid. In a 100-mL round bottom flask, succinic anhydride (1.4 g, 14.0 mmol) and $AlCl_3$ (5.6 g, 42.0 mmol) were dissolved in dry DCM (50 mL) at 0 °C, and 2-(9*H*-fluoren-9-yl)ethyl acetate (3.5 g, 14.0 mmol) dissolving in DCM (50 mL) was added dropwise over 20 min. The mixture was stirred at ambient temperature for 24 h. The reaction mixture was cooled at 0 °C with an ice bath and quenched with 1M aqueous solution of HCl until pH = 1. The reaction mixture was extracted with ethyl acetate (40 mL) 3 times. The organic layer was washed with 1M aqueous solution of HCl (20 mL) 3 times with brine (20 mL). The solution was dried over Na_2SO_4, and concentrated by rotary evaporation. Recrystallization from acetone afforded 3.8 g (79%) of products as a white solid. ^{1}H NMR (500 MHz, CD_3OD): δ 8.21 (s, 1H), 8.07 (d, *J* = 8.0, 1H), 7.90 (m, 2H), 7.61 (m, 1H), 7.39-7.44 (m, 2H), 4.19 (t, *J* = 5.7, 1H), 3.86-3.95 (m, 2H), 3.39 (t, *J* = 6.3, 2H), 2.74 (t, *J* = 6.3, 2H), 2.48 (q, *J* = 6.6, 2H), 1.75 (s, 3H). ^{13}C NMR (125 MHz, CD_3OD): δ 200.2, 176.7, 172.7, 149.1, 148.1, 147.3, 141.1, 136.8, 129.5, 128, 129.0, 128.6, 125.7, 125.2, 122.0, 120.9, 62.6, 46.0, 34.6, 32.0, 29.0, 20.5. High resolution ESI-MS: Calculated for $C_{21}H_{20}O_5Na^+$([M+Na]$^+$): 375.1208; obtained 375.1206.

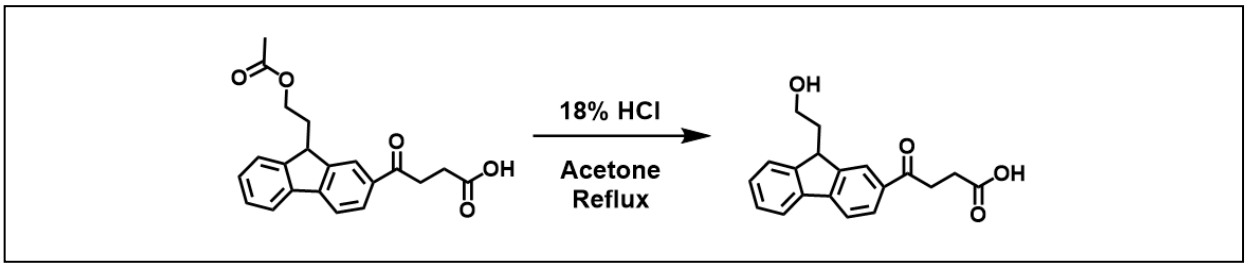

4-(9-(2-hydroxyethyl)-9*H*-fluoren-2-yl)-4-oxobutanoic acid. In a 100-mL round bottom flask, 4-(9-(2-acetoxyethyl)-9*H*-fluoren-2-yl)-4-oxobutanoic acid (3.8 g, 10.8 mmol) was dissolved in acetone (30 mL), and 18 wt % HCl (15 mL) was added. The mixture was refluxed for 5 h. Acetone was removed under vacuum, and solid was collected by filtration and washed with water and ethyl ether. Recrystallization from acetone afforded 2.0 g (60%) of the product as a white solid. ^{1}H NMR (500 MHz, $(CD_3)_2SO$): δ 12.2 (s, 1H), 8.19 (s, 1H), 7.96-8.05 (m, 3H), 7.65 (m, 1H), 7.39-7.45 (m, 2H), 4.18 (t, *J* = 6.5, 1H), 3.49 (t, *J* = 7.0, 2H), 3.32 (t, *J* = 6.3, 2H), 2.61 (t, *J* = 6.3, 2H), 1.99-2.13 (m, 2H). ^{13}C NMR (125 MHz, $(CD_3)_2SO$): δ 198.1, 173.9, 148.6, 147.5, 144.9, 139.1, 135.1, 128.2, 127.4, 127.2, 124.8, 124.0, 121.1, 120.0, 58.2, 44.0, 35.9, 33.2, 28.0. High resolution ESI-MS: Calculated for $C_{19}H_{18}O_4Na^+$([M+Na]$^+$): 310.1103; obtained 333.1100.

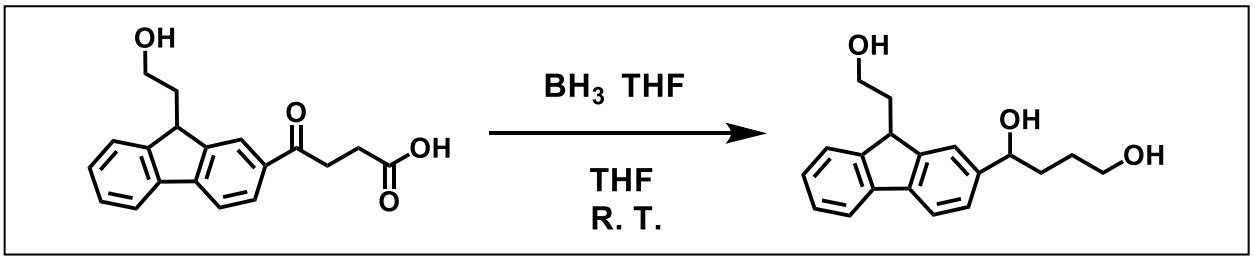

1-(9-(2-hydroxyethyl)-9*H*-fluoren-2-yl)butane-1,4-diol. In a 500-mL round bottom flask, 4-(9-(2-hydroxyethyl)-9*H*-fluoren-2-yl)-4-oxobutanoic acid (2.0 g, 6.5 mmol) was dissolved in THF (40 mL). The flask was purged with argon and cooled to 0 °C with an ice bath. 1M Borane tetrahydrofuran complex (19 mL, 19 mmol) in THF solution was added dropwise over 15 min. The mixture was stirred at ambient temperature for 12 h. After 12 h, the reaction was cooled to 0 °C and methanol (5 mL) and H_2O (10 mL) were added to quench the reaction. The organic solution was removed under vacuum. The reaction mixture was extracted with ethyl acetate (25 mL) 3 times. The combined organic layer was washed with brine (25 mL). The solution was dried over $MgSO_4$, and concentrated using a rotary evaporator. The crude product was purified by flash chromatography eluting with 7% (v/v) MeOH in DCM and resulted in 1.1 g (56%) of product as a white powder. ^{1}H NMR (500 MHz, CD_3OD): δ 7.75 (m, 2H), 7.54-7.57 (m, 2H), 7.26-7.37 (m, 3H), 4.72 (t, *J* = 7.2, 1H), 4.08 (m, 1H), 3.51-3.61 (m, 4H), 2.18 (m, 2H). 1.85 (m, 2H), 1.67 (m, 1H), 1.55 (m, 1H). ^{13}C NMR (125 MHz, CD_3OD): δ 148.6, 145.5, 142.0, 141.4, 128.1, 127.9, 126.3, 126.2, 125.5, 123.2, 120.7, 120.6, 120.5, 75.3, 62.9, 60.2, 45.5, 37.3, 36.9, 30.1. High resolution ESI-MS: Calculated for $C_{19}H_{22}O_3Na^+$([M+Na]$^+$): 321.1467; obtained 321.1467.

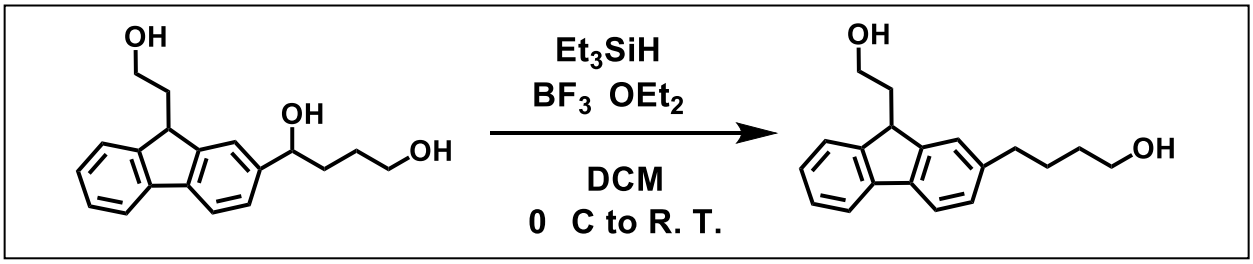

4-(9-(2-hydroxyethyl)-9*H*-fluoren-2-yl)butan-1-ol. In a 25-mL round bottom flask, 1-(9-(2-hydroxyethyl)-9*H*-fluoren-2-yl)butane-1,4-diol (0.39 g, 1.3 mmol) and Et_3SiH (0.43 mL, 2.6 mmol) were dissolved in dry DCM (3 mL) at 0 °C with an ice bath under nitrogen, and $BF_3{\cdot}Et_2O$ (0.3 mL) was added all at once to the reaction mixture. The mixture was stirred at 0 °C for 30 min. H_2O (2 mL) was added to reaction mixture to quench the reaction and the reaction mixture was extracted with DCM (5 mL) 3 times. The combined organic layer was washed with brine (5 mL). The solution was dried over $MgSO_4$, and concentrated using a rotary evaporator. The crude product was purified by flash chromatography eluting with 50% (v/v) ethyl acetate in hexane and resulted in 92 mg (25%) of product as a colorless liquid. ^{1}H NMR (500 MHz, $CDCl_3$): δ 7.72 (d, *J* = 7.5, 1H), 7.66 (d, *J* = 7.7, 1H), 7.51 (d, *J* = 7.4, 1H), 7.36 (m, 2H), 7.28 (t, *J* = 7.4, 1H), 7.19 (d, *J* = 7.7, 1H), 4.09 (t, *J* = 5.8, 1H). 3.67 (t, *J* = 6.5, 2H), 3.59 (t, *J* = 6.7, 2H), 2.73 (t, *J* = 7.6, 2H), 2.30 (q, *J* = 7.6, 2H), 1.75 (m, 2H), 1.63 (m, 2H). ^{13}C NMR (125 MHz, $CDCl_3$): δ 147.2, 146.8, 141.6, 141.1, 138.9, 127.6, 127.2, 126.7, 124.6, 124.5, 119.9, 119.8, 62.9, 60.4, 44.6, 36.0, 35.9, 32.5, 27.9. High resolution ESI-MS: Calculated for $C_{19}H_{23}O_2^+$([M+H]$^+$): 283.1698; obtained 283.1695.

General synthetic procedure of linear polymer 1. In a 5-mL glass vial, monomer **8** (27 mg, 0.1 mmol) was dissolved in dry NMP (0.2 mL) at room temperature. Hexamethylene diisocyanate (16 μL, 0.1 mmol) and dibutyltin dilaurate (5 μL, 0.008 mmol) were added in sequence. The mixture was stirred at room temperature for 24 h. Benzyl alcohol (10 μL) was added and stirred for another 1 h. The reaction mixture was precipitated in ethyl ether (8 mL), and the precipitate was isolated by centrifugation. This process was repeated 3 times. The polymer was dissolved with 50% (v/v) methanol in DCM (2 mL) and was precipitated in ethyl ether (8 mL), and the precipitate was isolated by centrifugation. This process was repeated 3 times. The purified precipitate was dried under high vacuum to afforded 32 mg (75%) of product as a white solid. GPC analysis (DMF): Mn = 22 kDa; Mw = 46 kDa; PDI = 2.1.

General synthetic procedure of control polymer 1c. In a 5-mL glass vial, control monomer **9** (28 mg, 0.1 mmol) was dissolved in dry NMP (0.2 mL) at room temperature. Hexamethylene diisocyanate (16 μL, 0.1 mmol) and dibutyltin dilaurate (5 μL, 0.008 mmol) were added in sequence. The mixture was stirred at room temperature for 24 h. Benzyl alcohol (10 μL) was added and stirred for another 1 h. The reaction mixture was precipitated in ethyl ether (8 mL), and the precipitate was isolated by centrifugation. This process was repeated 3 times. The polymer was dissolved with 50% (v/v) methanol in DCM (2 mL) and was precipitated in ethyl ether (8 mL), and the precipitate was isolated by centrifugation. This process was repeated 3 times. The purified precipitate was dried under high vacuum to afforded 31 mg (70%) of product as a white solid. GPC analysis (DMF): Mn = 11 kDa; Mw = 28 kDa; PDI = 2.6.

General synthetic procedure of polymeric network 11. In a 5-mL glass vial, Fmoc triol monomer **6** (142

mg, 0.5 mmol) was dissolved in dry NMP (0.5 mL) at room temperature. Hexamethylene diisocyanate (88 μL, 0.55 mmol) and dibutyltin dilaurate (40 μL, 0.064 mmol) were added in sequence. Finally, 0.05 mL NMP bromothymol blue indicator stock solution (1 mg/1 mL) was added and the solution was stirred for 15 minutes at room temperature. The solution was quickly transferred to circular PTFE mold (2.2 cm diameter and 500 μm thickness) and covered by glass with non-stick paper to control the thickness (500 μm), reacting at room temperature in the vacuum oven under nitrogen for 24 h.

3. Monomer Characterization

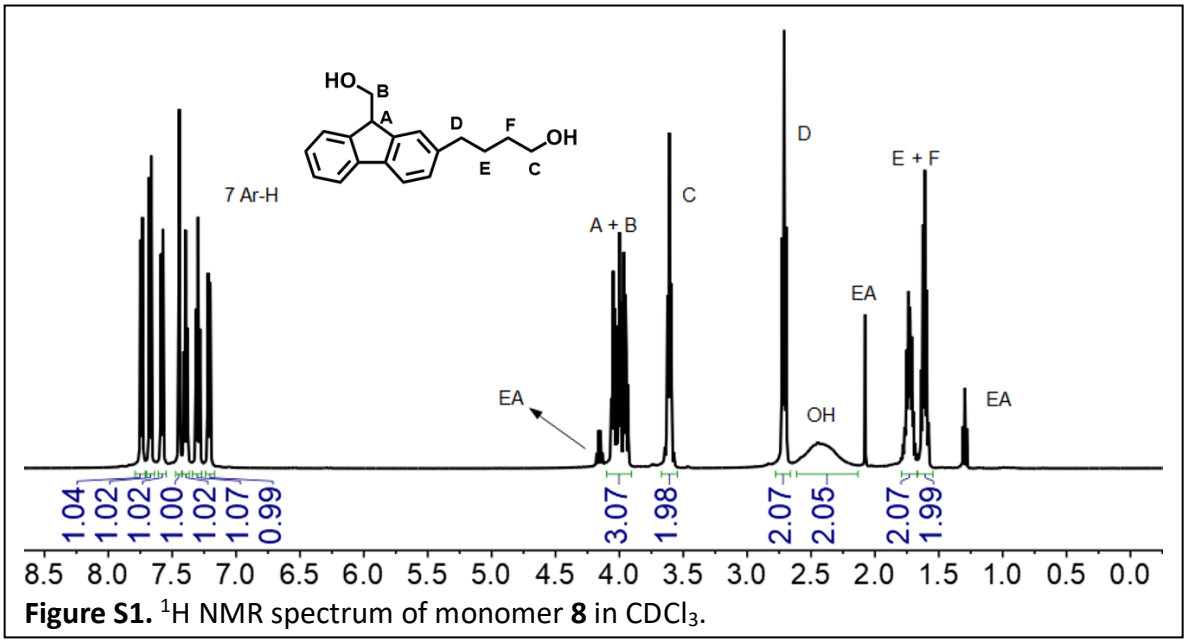

Figure S1. ^{1}H NMR spectrum of monomer **8** in $CDCl_3$.

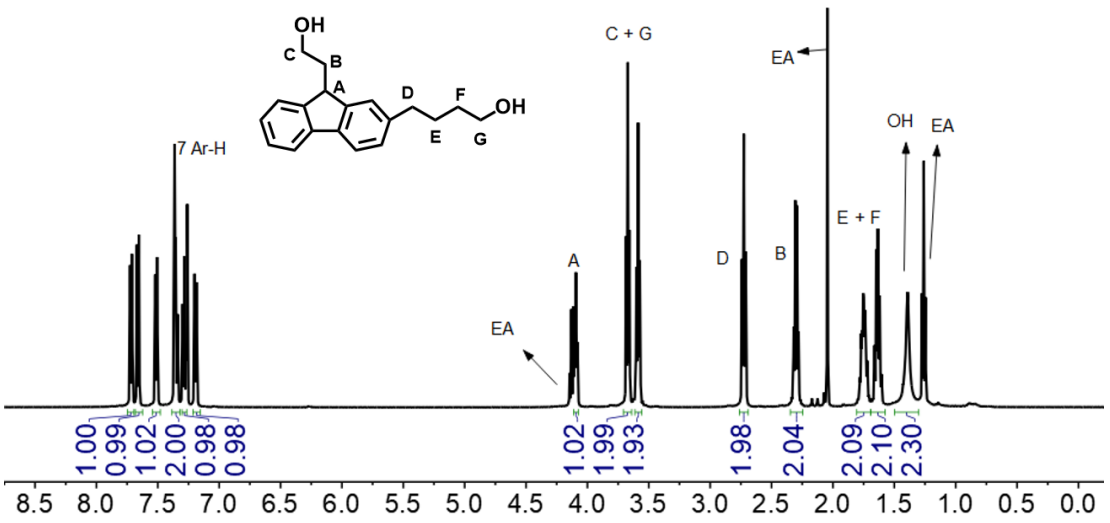

Figure S3.[1]H NMR spectrum of control monomer **9** in $CDCl_3$.

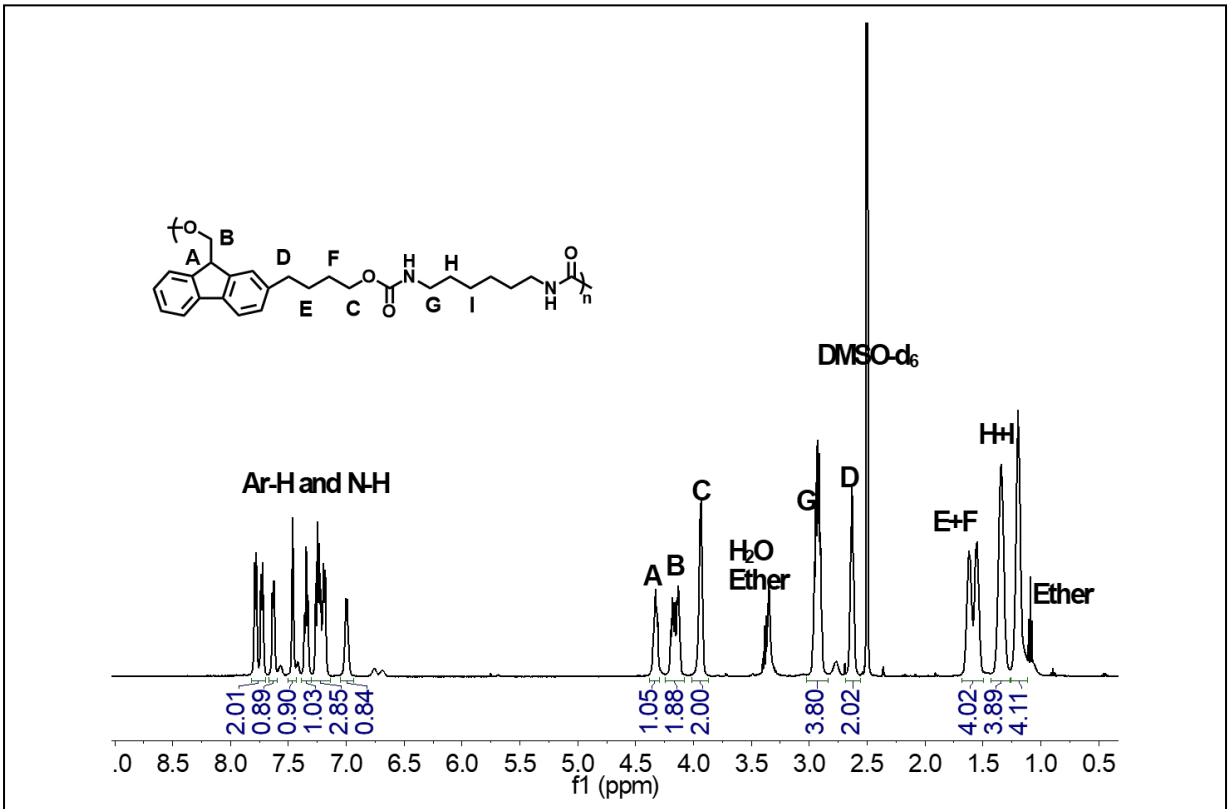

Figure S2. Representative structure and [1]H NMR spectrum of polymer **1** in DMSO-d_6

4. Polymer Characterization

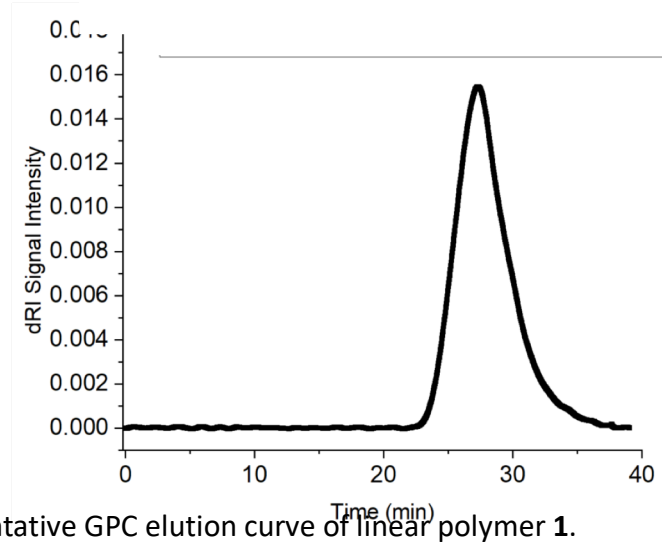

Figure S4. Representative GPC elution curve of linear polymer **1**.

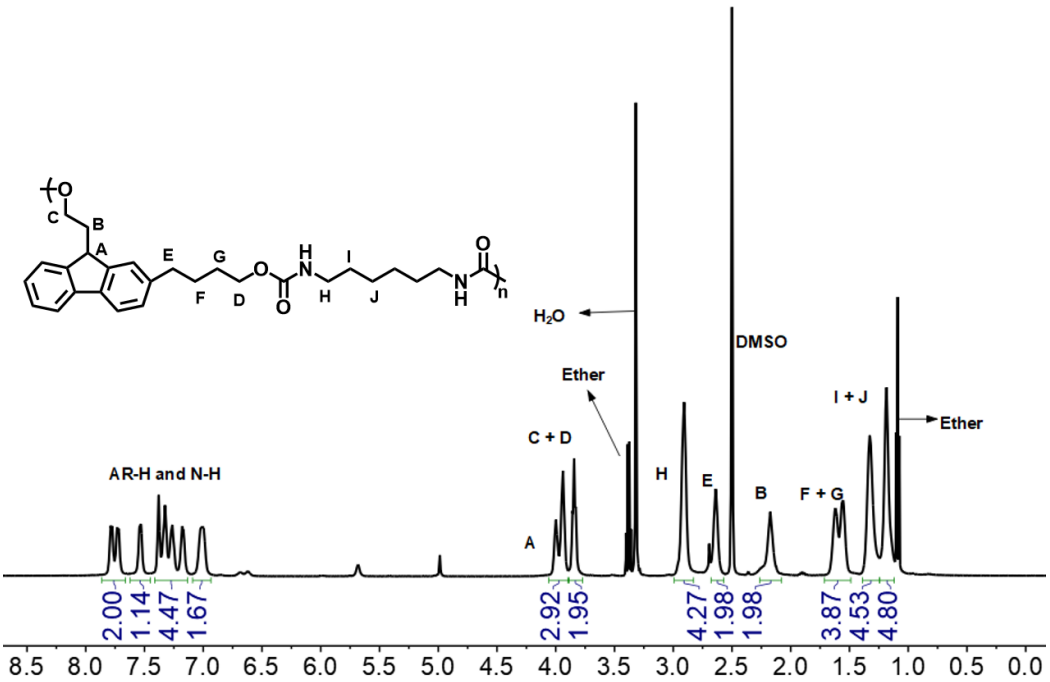

Figure S5. Representative structure and ^{1}H NMR spectrum of control polymer **1c** in DMSO-d_6

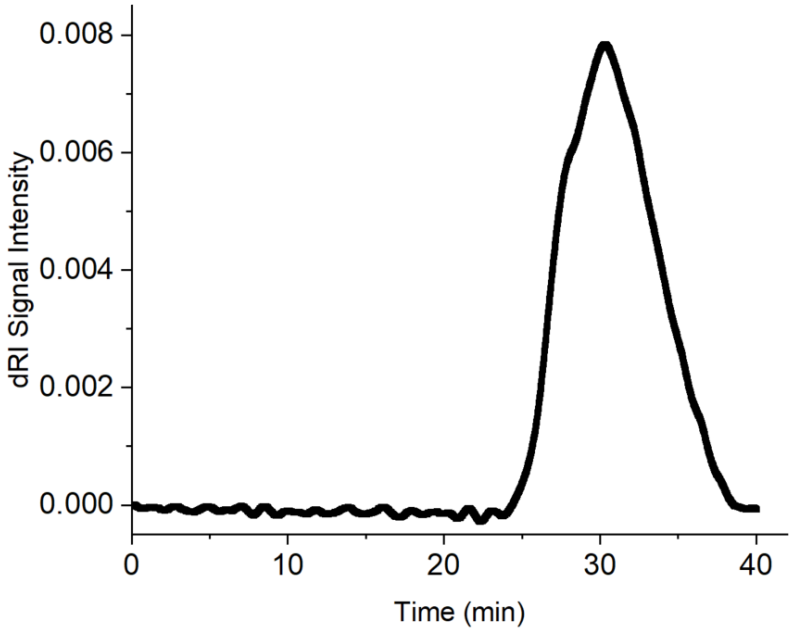

Figure S6. Representative GPC elution curve of control polymer **1c**.

5. GPC and NMR Degradation Study of Linear Polymer

General procedure for the base-induced degradation of polymers and the MW analysis by GPC.

In a 5 mL vial, 1 mL linear polymer **1** or **1c** (10 mg/ mL) was dissolved in DMF with 0.1 M LiBr. The solutions were passed through 0.45 μm syringe filters and 38 μL 30 mM hexylamine in DMF solution was added to trigger the degradation. The degradation of polymer was allowed to proceed in a small vial for

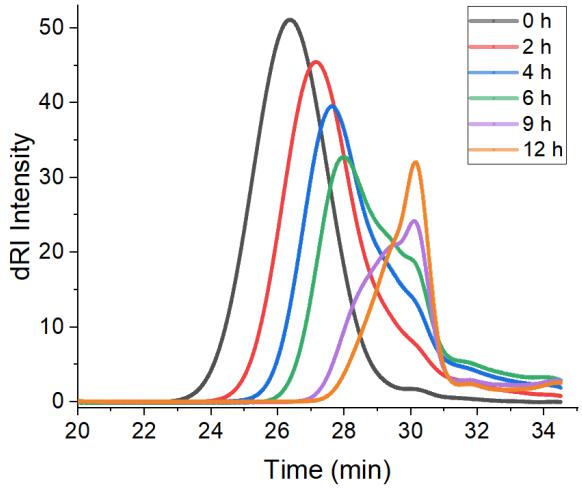

Figure S7. Representative GPC elution curve of polymer **1** with addition of 5% hexylamine (according to total degradable Fmoc moiety concentration instead of polymer concentration) over 12 h.

12 h for linear polymer **1** and 24 h for control polymer **1c**. At different time point, 50 μL of polymer solution was taken out from the small vial and injected to the GPC for polymer MW analysis directly.

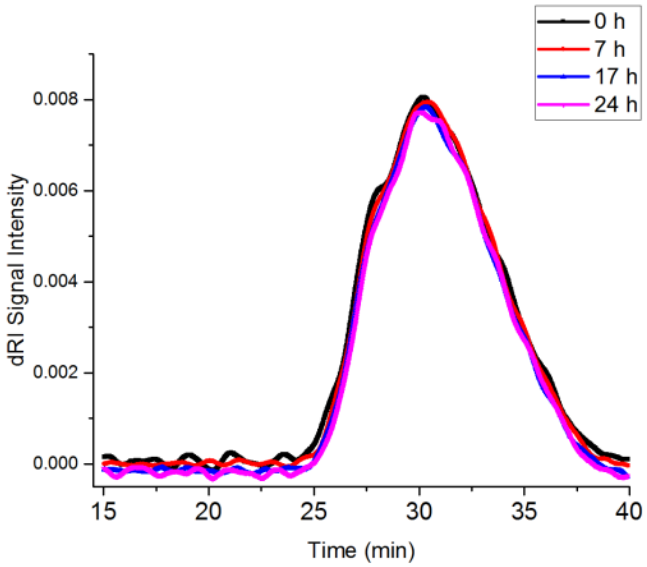

Figure S8. Representative GPC elution curve of **control polymer 1c** with addition of 5% hexylamine (according to repeating unit concentration instead of polymer concentration) over 24 h.

General procedure for the ^{1}H NMR analysis of base-induced degradation of polymers.

In a 5-mL small vial, around 5.26 mg polymer samples for NMR degradation studies were dissolved in 0.3 mL DMSO-d_6 solution and 0.2 mL of a 12 mM solution of acetanilide in DMSO-d_6 was added as an internal standard. The concentration of the repeating units of polymer was estimated to be 24 mM in DMSO based on the amount added and the repeating unit MW. Varying amounts of 30 mM hexylamine in DMSO-d_6 stock solution was added to the small vial to trigger the degradation. The solution was immediately transferred to an NMR tube and capped. The degradation was monitored at room temperature at different time point over 15 h. The degradation percentage was calculated by integrating the signal at δ 4.33 ppm or 6.25 ppm with respect to the signal at 2.03 ppm (acetanilide as internal standard, constant proton signal). These experiments were run with addition of varying concentration of hexylamine as trigger and the data was fitted to equation S3 to obtain rate constants.

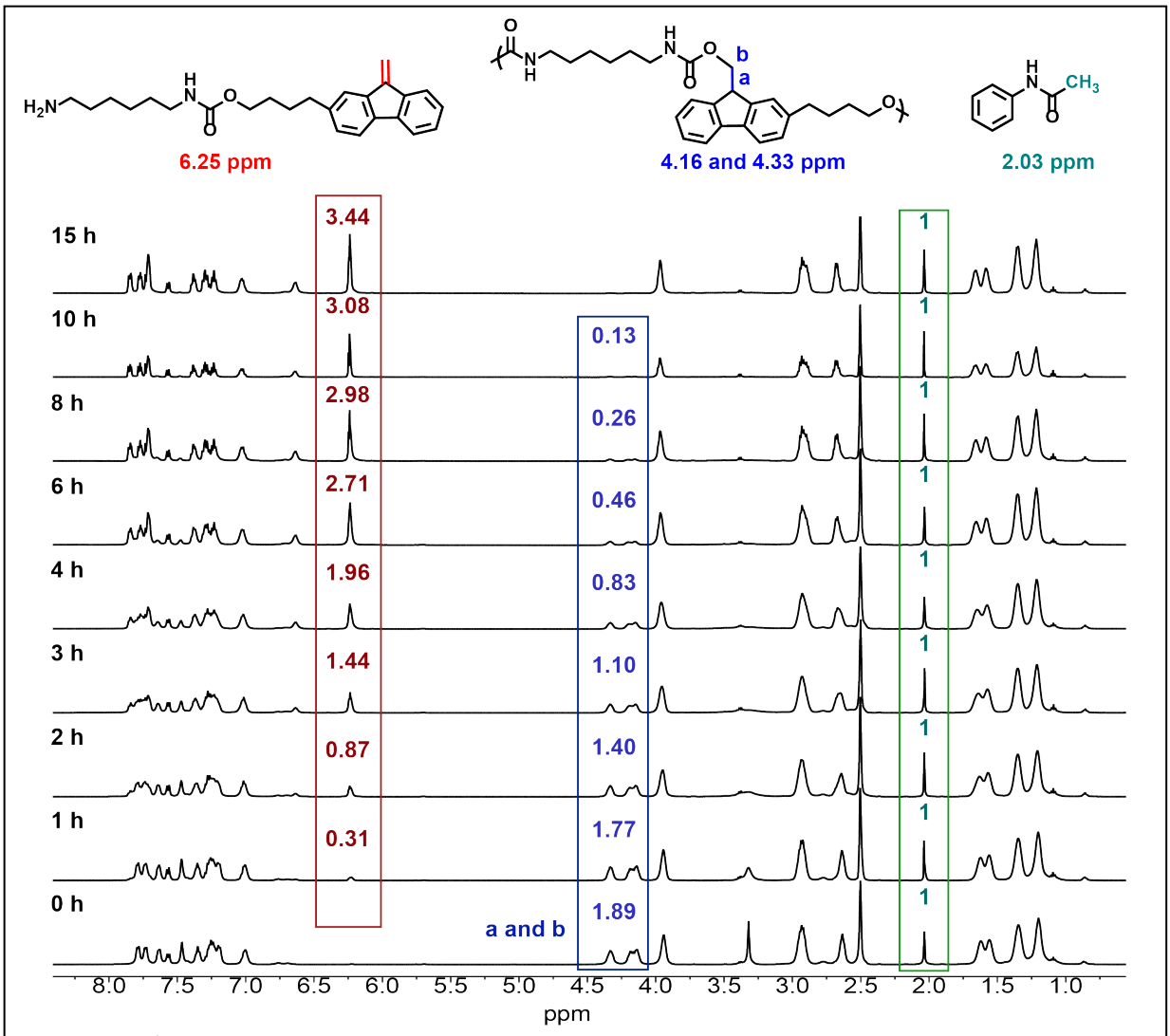

Figure S9. ^{1}H NMR analysis of the degradation kinetics of polymer **1** in a 24 mM solution In DMSO-d_6 with addition of 5% hexylamine corresponding to repeating unit concentration.

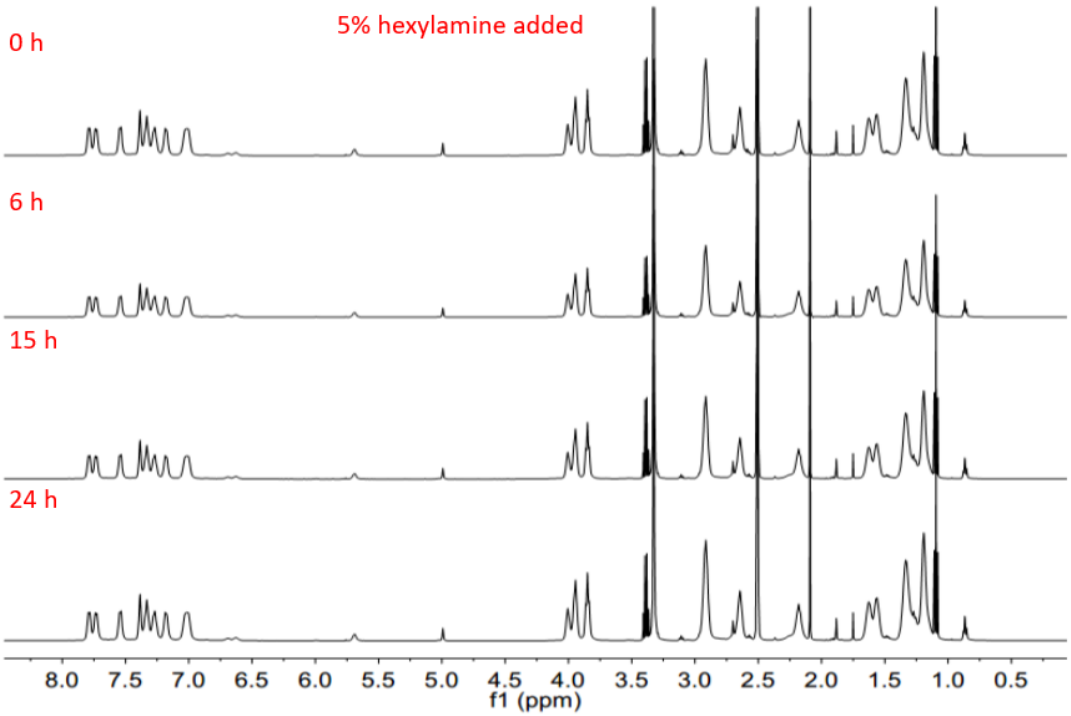

Figure S10. ^{1}H NMR degradation study of control polymer **1c** with addition of 5% hexylamine corresponding to repeating unit concentration.

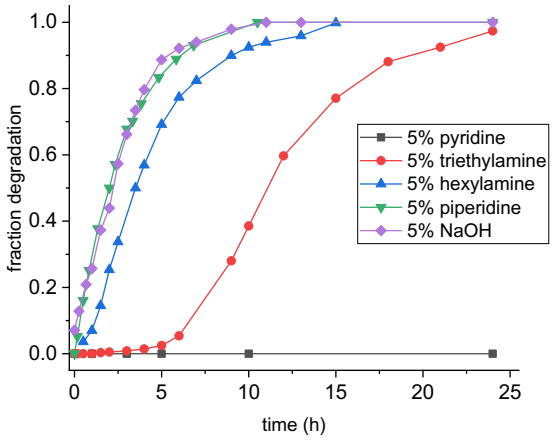

Figure S11. ^{1}H NMR degradation of **1** over time with different base as trigger. 5 mol% different types of base trigger(pyridine, triethylamine, hexylamine, piperidine, NaOH) corresponding to repeating unit concentration was added and the fraction degradation was calculated from ratio of signals at δ 6.25 or 4.25 ppm (alkene product or a/b protons of starting polymer) and internal standard at 2.03 ppm. Lines connecting the points are to guide the eyes. When it comes to NaOH degradation study, 120 mM NaOH stock solution was firstly made in D_2O solvent and added to the DMSO-d_6 polymer solution to trigger the degradation.

6. LCMS Analysis of the Degradation Product

The degradation product from linear polymer **1** in DMSO solution was precipitated in water and washed with water. The product was transferred to a vial and put in a lyophilizer overnight. An aliquot (2 μL) of the reaction mixture was diluted with acetonitrile and the resulting solution was injected into an analytical reversed-phase HPLC coupled to a mass spectrometer. The mobile phase used was a mixture of 0.1% TFA in H_2O (A) and 0.1% TFA in CH_3CN (B). The flow rate was 0.4 mL / min.

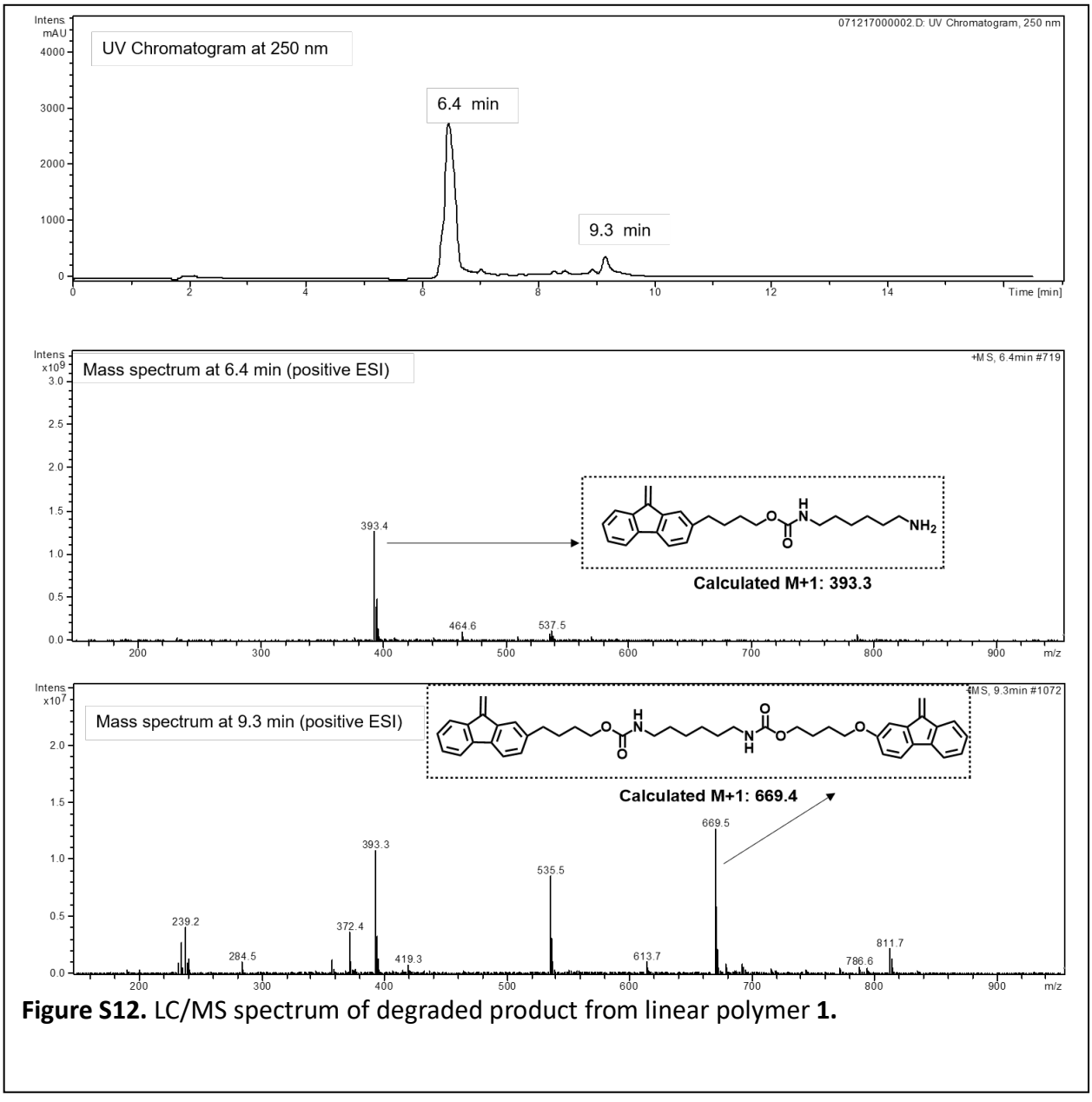

Figure S12. LC/MS spectrum of degraded product from linear polymer **1.**

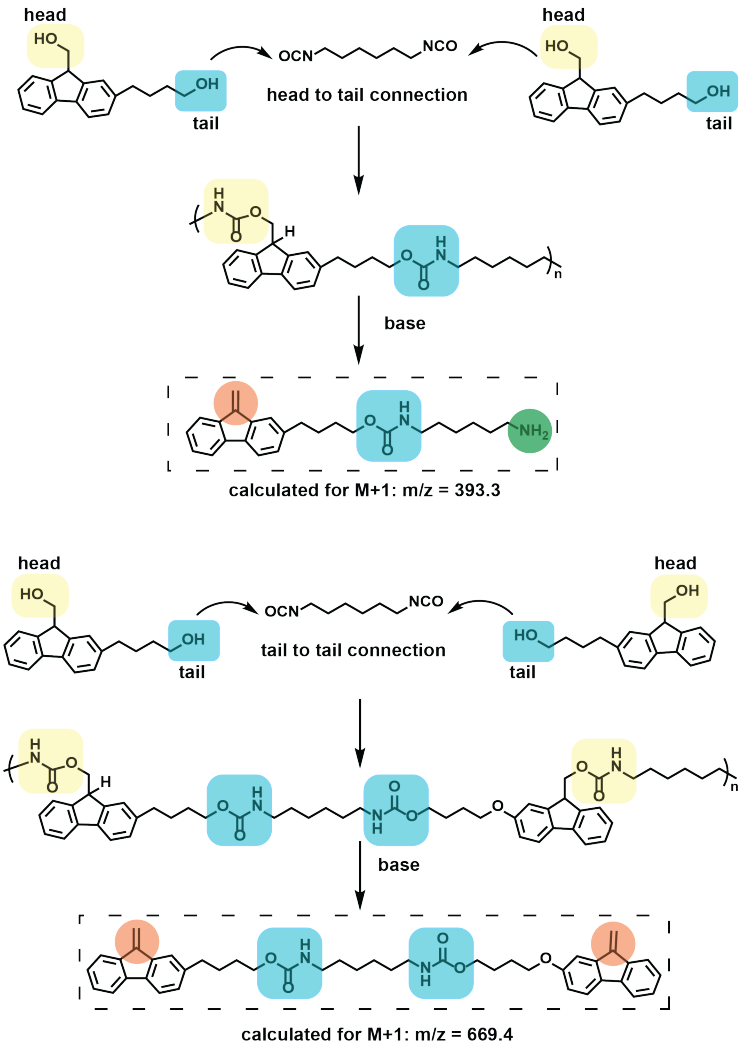

Figure S13. Two types of repeating unit structures are seen in the LC/MS.

7. NMR Degradation Autocatalytic Kinetic Analysis

The previously reported method was used for the degradation kinetic study.[2-5] The reaction rate can be represented as

$$r = k_1[R] + k_2[R][P] \text{ , (S1)}$$

Where R represents the reactant, P represents the product, and k_1 and k_2 represent individually the rate constants of non-autocatalytic and autocatalytic mechanisms. This equation can be converted to

$$-\frac{dc}{dt} = k_1 c + k_2 c(c_0 - c) \text{ , (S2)}$$

where c is the concentration of the degradable component with its initial concentration value being c_0. This ordinary different equation can be solved by direct integration.[5] After some rearrangement and simplification this results in the rate law

$$\frac{c}{c_0} = \frac{k_1 + k_2 c_0}{k_1\, e^{(k_1 + k_2 c_0)t} + k_2 c_0} \text{ (S3)}$$

which is the final equation to represent reaction conversion as a function of time. The S3 equation can be utilized to fit k_1 and k_2 by least-squares regression of the normalized amount of non-degraded Fmoc. For polymer samples, it should be noted that the concentration must be calculated from the moles of total degradable agents in the solution rather than simply the moles of polymer. The c_0 values used were 0.024 M for 0.5% trigger, 0.022 M for 1% trigger, 0.024 M for 5% trigger.

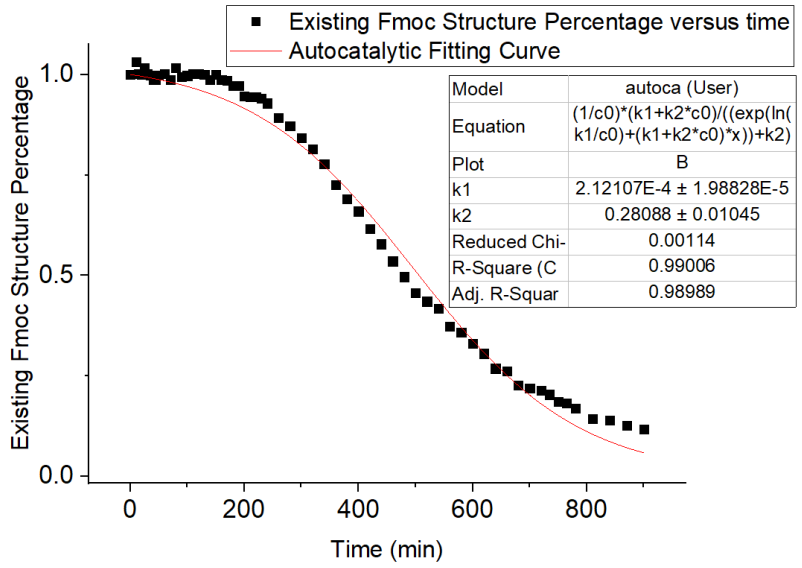

Figure S14. Representative data fit for the disappearance of proton A and proton B in ^{1}H NMR of polymer **1** with addition of 0.5% hexylamine as trigger. The repeating unit concentration is 24 mM solution in DMSO-d_6 at 25 °C. The red line represents the fit of the data to equation S4 (R^2 = 0.990).

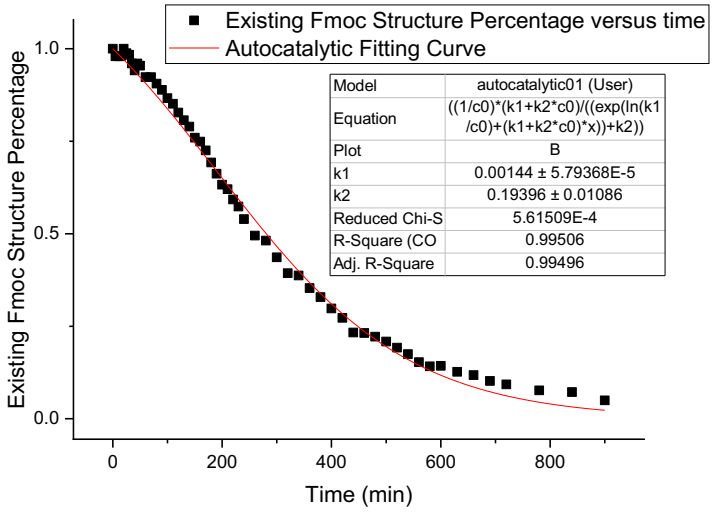

Figure S15. Representative data fit for the disappearance of proton A and proton B in ^{1}H NMR of polymer **1** with addition of 1% hexylamine as trigger. The repeating unit concentration is 22 mM solution in DMSO-d_6 at 25 °C. The red line represents the fit of the data to equation S4 (R^2 = 0.995).

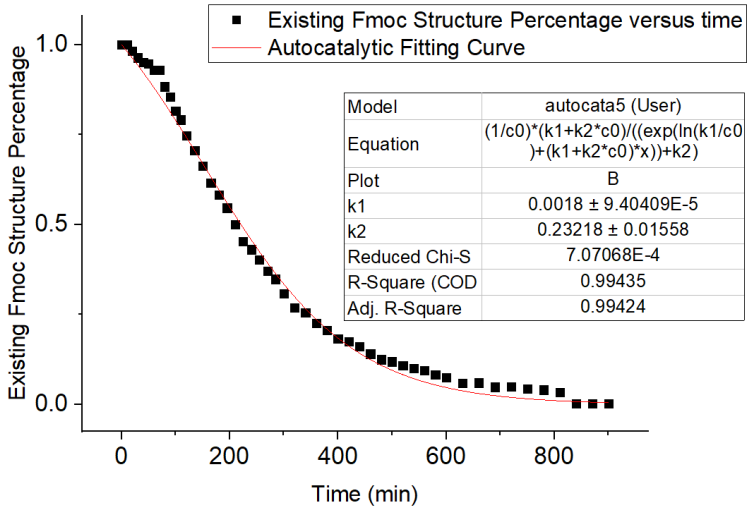

Figure S16. Representative data fit for the disappearance of proton A and proton B in ^{1}H NMR of polymer **1** with addition of 5% hexylamine as trigger. The repeating unit concentration is 24 mM solution in DMSO-d_6 at 25 °C. The red line represents the fit of the data to equation S4 (R^2 = 0.994).

8. Synthesis and Characterization of Polymeric Network

(a)

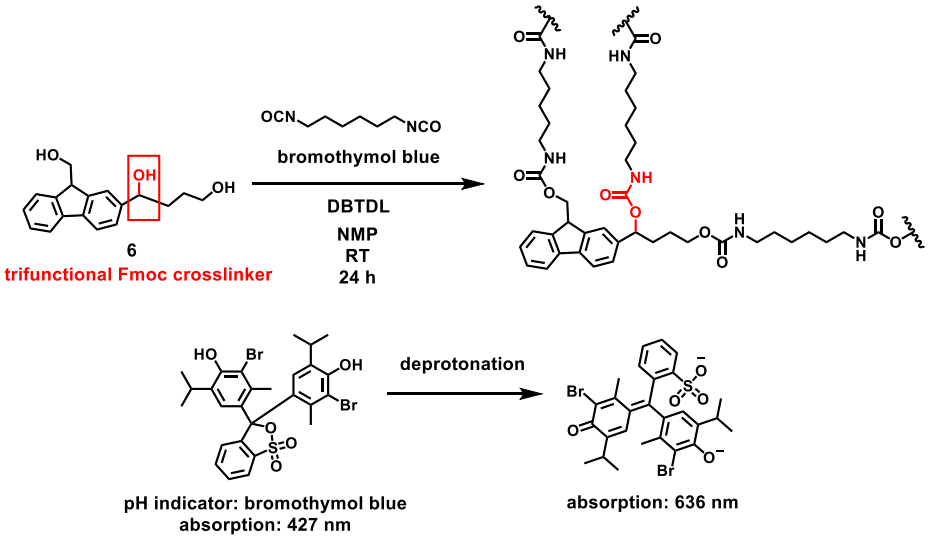

(b)

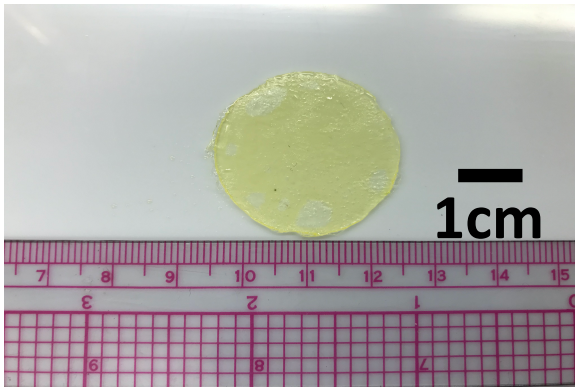

Figure S17. (a) Synthesis of base-generating self-amplifying degradable polymeric network **11**. (b) Visual observation of the organogel formed with 2.9 cm diameter and 500 µm thickness.

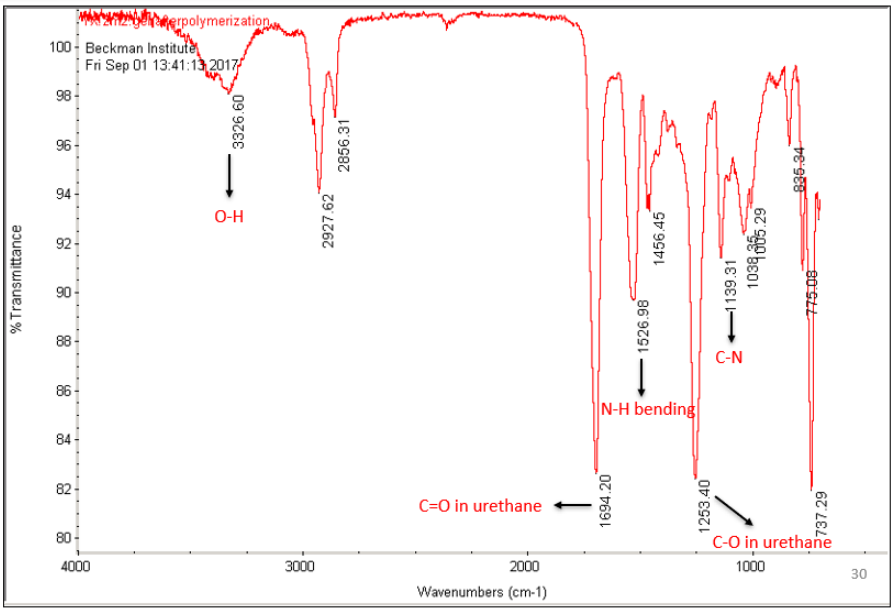

Figure S18. Attenuated total reflection IR spectrum of crosslinked polymer network **11**.

9. Degradation Study of Degradable Polymeric Network.

The polymeric network was immersed in 5 mL bromothymol blue stock solution in NMP (1mg / mL) to swell for 3 h. The weight of the polymeric network after absorbing solvent was 740 mg. A cyclindrical punch with 29 mm diameter was used to trim the swelled polymeric organogel. And a smaller punch with 2.2 mm diameter was used to make a small hole in the center of the round polymeric organogel for base addition. The gel material was placed onto a 29 mm diameter Teflon mold. 2 μL of 180 mM hexylamine in NMP solution was added in the middle of the small hole and the photos was taken by camera every 10 min. The fraction of color change (the area with color change to green blue) of the network versus time plot was quantified by Image-Pro-Plus software.

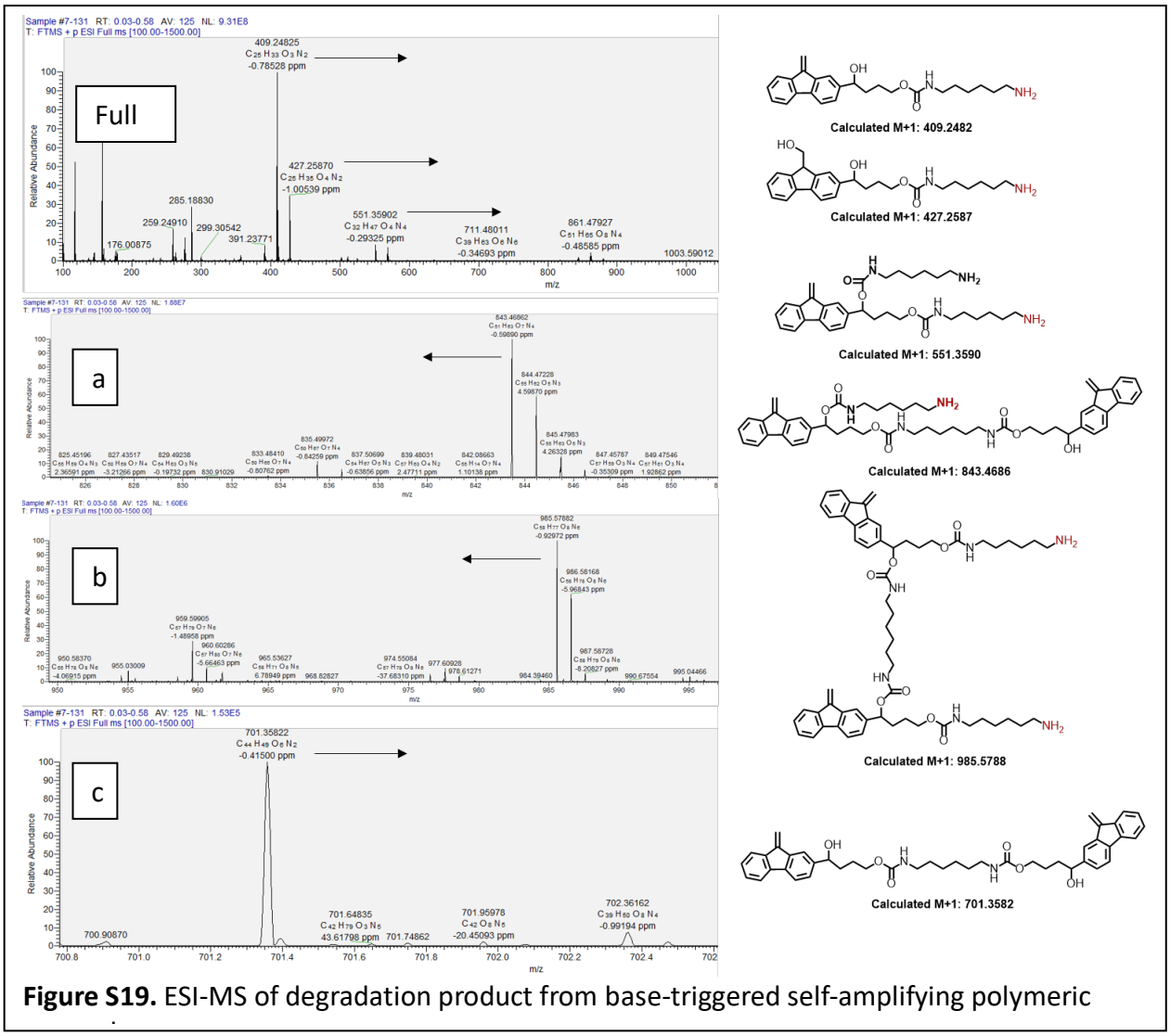

Figure S19. ESI-MS of degradation product from base-triggered self-amplifying polymeric

The protocol for processing the photos through Image-Pro-Plus:

(**1**) Load the gel degradation photos at different time point in Image-Pro-Plus. From the Enhance menu, select the Equalize submenu, and then select the Best Fit command. Select the Apply Contrast command from the Enhance menu and click OK when the Apply Contrast dialog box appears. This operation

enhanced the contrast for every gel degradation photo.
(**2**) Perform non-degraded yellow color segmentation and degraded non-yellow color segmentation: In this step, both the non-degraded yellow area of the gel and degraded non-yellow area of the gel are selected and counted by using the color cube method of separation. (a) Select the *Count/Size* option from the *Measure* menu. (b) Click the Manual radio button and T*he Select Colors* … button is now accessible. Click on t*he Select Colors*… button and click on the *Color Cube Based* t*ab*, which separates the non-degraded yellow area of gel that are to be counted and measured. Click on the *Eyedropper* button in the *Select* Image group box. Move the cursor on to several yellow non-degraded areas in the image to perform segmentation and then click the left mouse button to these several yellow non-degraded area and it will automatically selects all other similar non-degraded yellow color areas in the photo. Image-Prop Plus takes the highlighted non-degraded yellow areas to segment and turns them red as shown below. Similarly, color segmentation could be performed for degraded non-yellow area and it was highlighted in purple color shown below. Click Close. At this point, the non-degraded yellow area and degraded non-yellow area have been identified.
(**3**) Define an Area of Interest (AOI) in the gel degradation photos. (a) Select the Ellipse AOI tool. Use

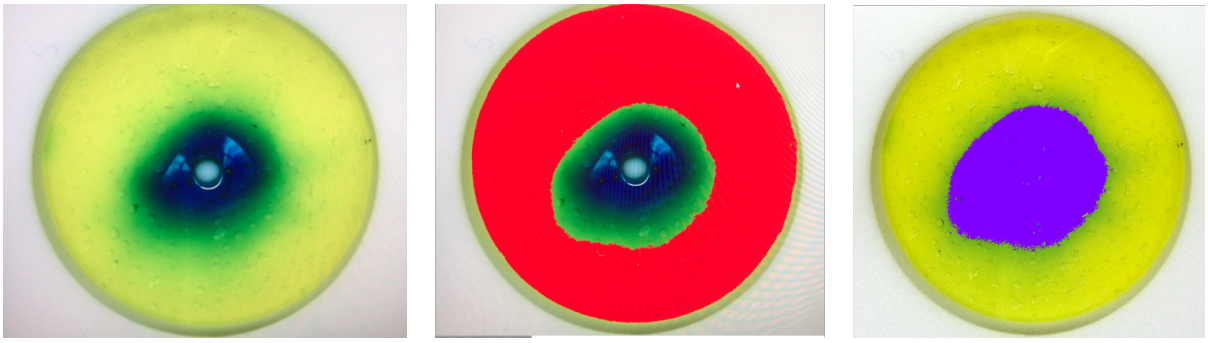

Figure S20. Example of peforming non-degraded yellow area color and degraded non-yellow area color segmentation.

the Ellipse AOI tool to generate a circle to circle around the circular gel material in the photo.
(**4**) Count the non-degraded yellow area and degraded non-yellow area. (a) Click on *Count* in the *Count/Size* dialog box. (b) From the *Measure* menu in the *Count/Size* dialog box, select the *Select Measurements*… command. When the Select Measurements dialog box appears, you could see Area was the default. Click on *Measure*. From the *View* menu in the *Count/Size* dialog box, select the *Statistics* command. The Statistics window appears with the statistic data sheet for the image, including the non-degraded yellow *area and degraded non-yellow area.*

The more detailed quantification method could follow Chapter 8 (Color Segmentation) in instruction manual – Image-Pro Plus Version 5.1 for Windows. Quantification of the percentage of non-degraded yellow area in the total area could be calculated and the fraction of color change area versus time curve could be easily gained after simple mathematical conversion in Origin 8 software.

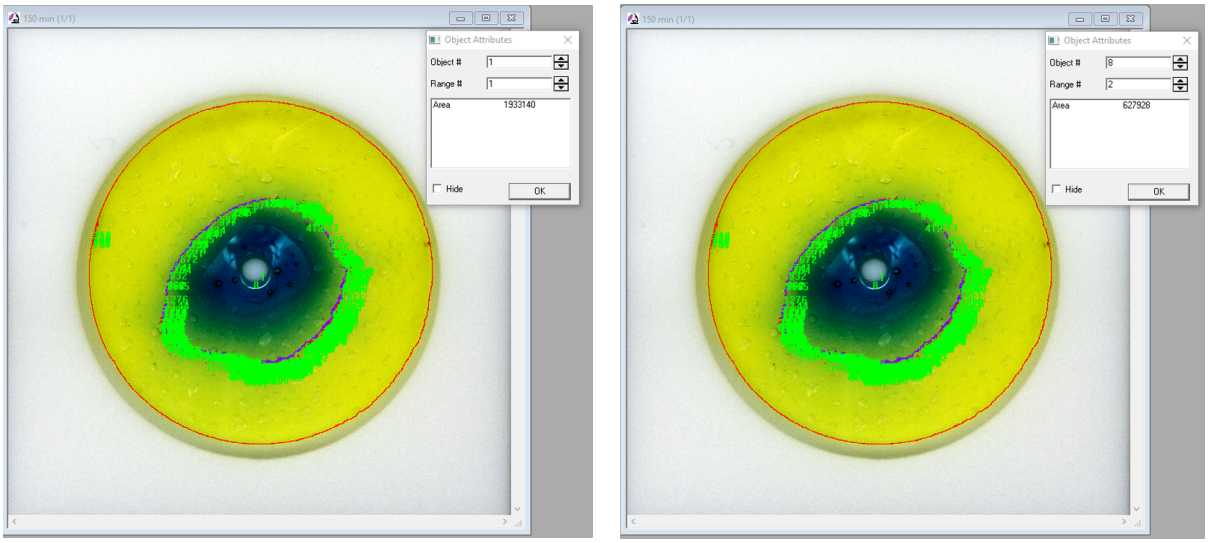

Figure S21. Example of counting the area of non-degraded yellow area(left) and degraded non-yellow area(right).

Once the gel just completely collapsed into solution, GPC and NMR was measured and compared to the result of them after 6 h. The result suggested that there were still oligomer existence in the solution once the gel collapsed into solution and the degradation could continue in the solution.

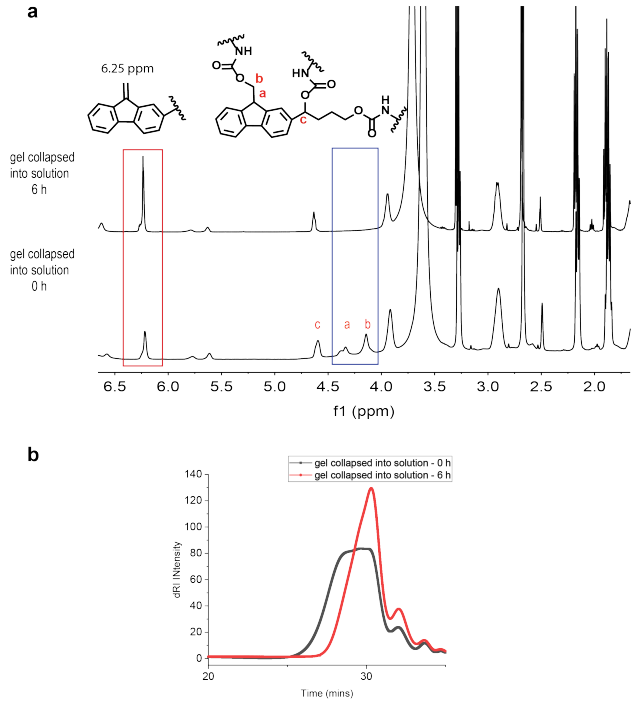

Fig. S22. (a) ^{1}H NMR spectra of gel degradation of **11** in DMSO-d_6 with 2 µL 180 mM hexylamine as trigger. Bottom: ^{1}H NMR taken once solid gel fully collapsed into solution, top: ^{1}H NMR taken for the gel degradation solution after 6 h.(b) GPC of **11** with addition of 2 µL 180 mM hexylamine as trigger. Black: GPC trace taken once solid gel fully collapsed into solution, red: GPC trace taken for gel degradation solution after 6 h. GPC was taken by directly dilution of the NMP degradation solution into DMF solution with LiBr to run.

10. Degradation of Polymeric Network Monitored by Rheology

Characterization of linear viscoelastic properties was performed on a combined motor/transducer DHR-3 rotational rheometer from TA instruments using a parallel-plate geometry with a diameter of 20 mm and Peltier temperature control. For rheological characterization, all gels were prepared at a nominal thickness of 1.5 mm for loading. During measurements, the gap was continuously varied to maintain a normal force of 0.5 ± 0.2 N to avoid edge fracture and maintain contact across the geometry. A low viscosity mineral oil was applied to the exposed surface of the gel to prevent evaporation. All samples were loaded onto the rheometer geometry at 25 °C and 5 μL 360 mM hexylamine NMP solution was added in the center of the gel, while the control experiment was conducted without base addition. To obtain the viscoelastic storage and loss moduli, G' and G'' respectively, samples were held at 25 °C and probed at an oscillatory strain amplitude of 2.5% at a frequency of 1 rad/s. This strain amplitude was in the linear deformation regime. For all samples, before any significant change in the moduli of the material, the ratio of G'' to G' (i.e. tan(δ) = G''/G') was always less than 0.1. For the samples that undergo a dramatic decrease in G', during and after the decrease, tan(δ) was always less than 1. G'' and tan(δ) are omitted from plots for clarity. Little frequency dependence was observed for any of the materials across the range of 0.1 to 30 rad/s. The experimental data was fitted to the autocatalytic rate equation to obtain rate constants.

The gray region in Fig. 4e indicates the range below which oscillatory shear modulus data cannot be trusted, since this corresponds to the low-torque limit of the instrument. Data in this region is usually noisy, and an estimate of the limits can be obtained from $G_{min} = \frac{T_{min} F_\tau}{\gamma_0}$, where F_τ is a geometry dependent conversion factor to go from torque signals (which is actually measured by the instrument) to stress, T_{min} is the low-torque limit of the instrument (specified by the manufacturer), and γ_0 is the strain amplitude employed in the experiment.[12] The minimum torque limit specified by TA instruments is 0.5 nNm, but as a rule of thumb, in order to have sufficient margin of safety, the actual limit used in the calculation was 10 times this, so we have used T_{min} = 5 nNm. Using this, the minimum shear (storage) modulus that can be measured is 0.17 Pa.

In the case of the organogel, k_1 and k_2 must be extracted from the normalized storage modulus. Using the phantom model of rubber elasticity[6,7] and assuming a network functionality of f = 3 (as expected for a bifunctional crosslinker), the plateau modulus G_0 and the number density of elastically active crosslinks (μ) are related by $G_0 = (\nu - \mu)k_BT = 0.5\mu k_BT$, where $\nu = \mu \times f/2$ is the number density of elastically active network strands and k_BT is the thermal energy scale.[8, 9, 10, 11] In the case of fitting G/G_0 (Given that $\mu = N_A c$),

$$c = \frac{2G}{k_B T N_A} \text{ and } c_0 = \frac{2G_0}{k_B T N_A} \quad \text{(S4)}$$

Substituting Equation S4 into S3,

$$\frac{G}{G_0} = \frac{k_1 + \frac{2k_2 G_0}{k_B T N_A}}{k_1 e^{(k_1 + \frac{2k_2 G_0}{k_B T N_A})t} + \frac{2k_2 G_0}{k_B T N_A}} \quad \text{(S5)}$$

Thus, for the degradation profile, k_1 and k_2 were found using least-squares regression of the normalized storage modulus (using Equation S5). The values from each triplicate measurement were averaged and reported. In addition, the organogel k_2 values calculated from storage modulus neglect the effects of loops

and other inactive cleavage sites. These could be accounted for in the rate equation by assuming a constant ratio of elastically inactive cleavage sites, $\phi = c^{inactive} / c^{active}$, where $c^{total} = c^{inactive} + c^{active}$. Equation S2 is true for c^{total} but can be rewritten to account for inactive crosslinking by substituting $c^{total} = (1 + \phi)c^{active}$. We have assumed that $\phi = 0$, so k_2 from our fit may be larger than the true rate constant by a factor of $1 + \phi$. In comparing the rates between systems, we found that the k_1/k_2c_0 value for all systems is << 1 as is characteristic of autocatalytic reactions.

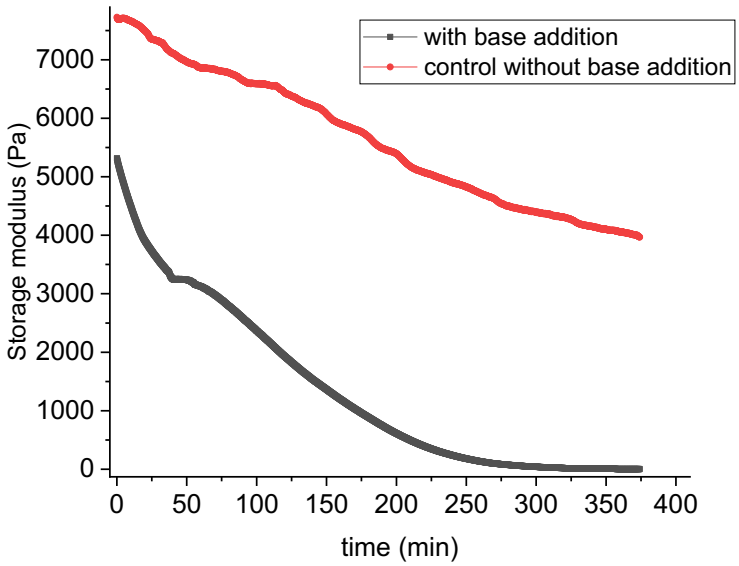

Figure S23. Storage modulus change for sample with 5µL 360 mM hexylamine base addition and control sample without base addition.

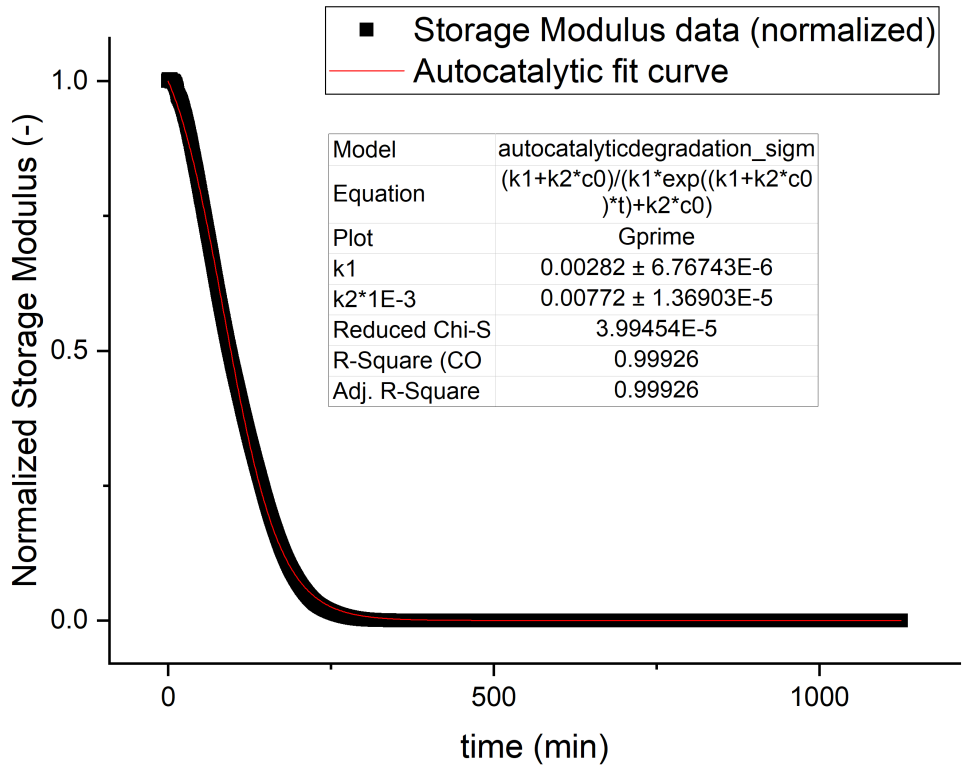

Figure S24. Representative example of fitting of the normalized storage modulus to the autocatalytic degradation equation.

Table of fitting data from triplicate experiment.

Experiment	k_1 (min^{-1})	k_2 (M^{-1} min^{-1})	k_2c_o (min^{-1})
Average	0.00209 ± 0.00114	3.68 ± 3.65	15.93 ± 5.26

11. Supplemental TGA of Polymer

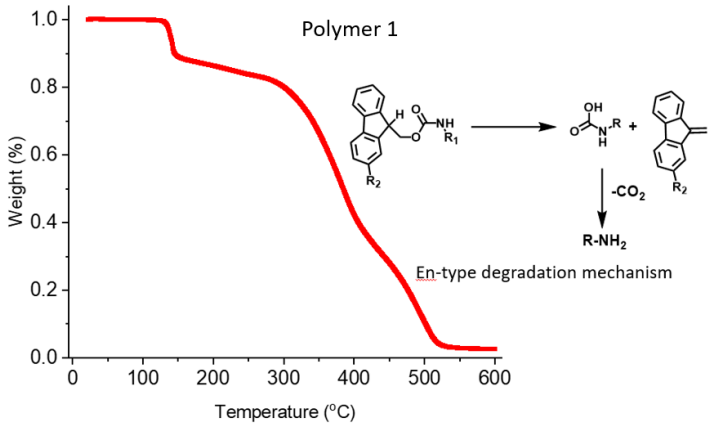

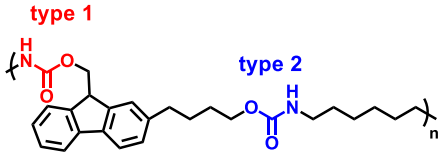

Figure S25. TGA data of linear polymer **1** with ramping temperature at the rate of 5°C/min. The temperature for 5% weight loss is 118 °C.

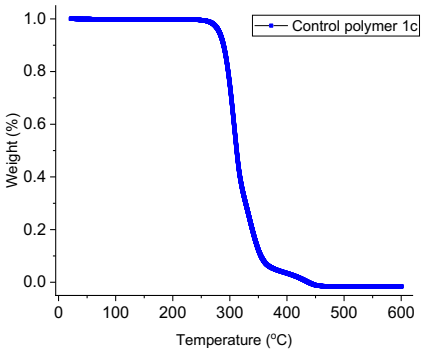

Figure S26. TGA data of linear control polymer **1c** with ramping temperature at the rate of 5°C/min. The temperature for 5% weight loss is 281 °C.

12. Supplemental DSC of Polymer

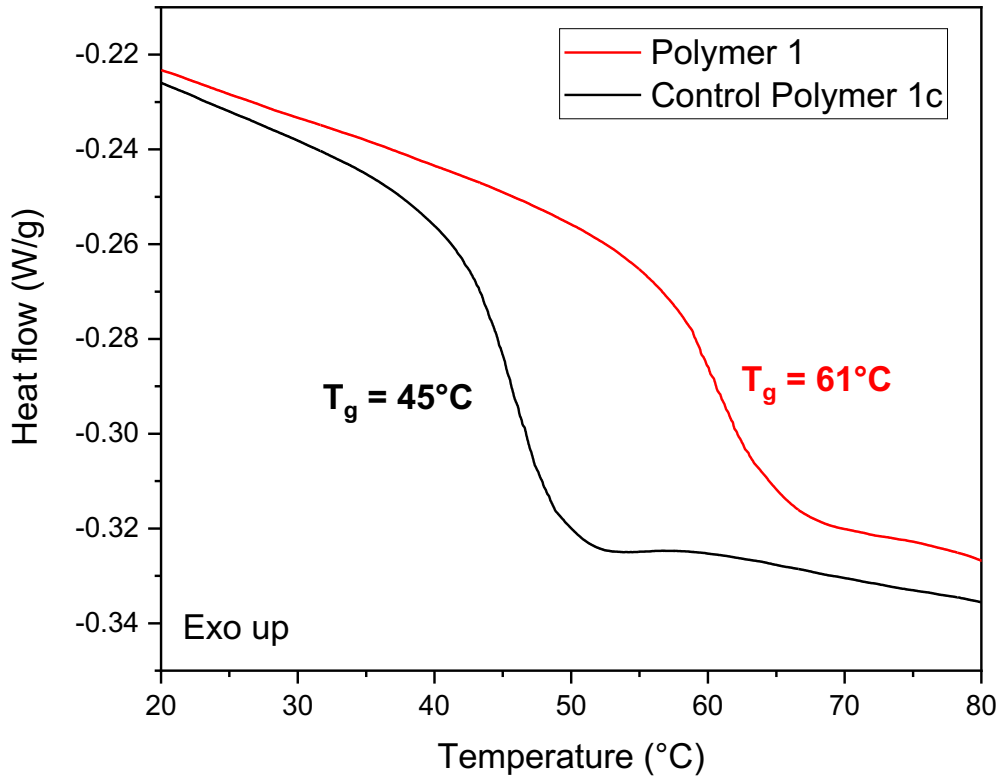

Figure S27. DSC of linear polymer **1** and control polymer **1c**. "Exo up" indicates that the direction of exothermic heat flow is up. T_g was calculated by half-height midpoint method on 2nd heating cycle with a heating rate is 5 °C/min.

13. References

1. J. Perumattam, C. Shao and W. L. Confer, *Synthesis,* 1994, **1994**, 1181-1184.
2. F. Mata-Perez and J. F. Perez-Benito, *J. Chem. Educ.,* 1987, **64**, 925-927.
3. J. F. Perez-Benito, *J. Phys. Chem. A,* 2011, **115**, 9876-9885.
4. O. P. Lee, H. Lopez Hernandez and J. S. Moore, *ACS Macro Lett.,* 2015, **4**, 665-668.
5. K. A. Miller, E. G. Morado, S. R. Samanta, B. A. Walker, A. Z. Nelson, S. Sen, D. T. Tran, D. J. Whitaker, R. H. Ewoldt, P. V. Braun and S. C. Zimmerman, *J. Am. Chem. Soc.,* 2019, **141**, 2838-2842.
6. P. J. Flory and J. Rehner, *J. Chem. Phys.,* 1943, **11**, 512-520.
7. H. M. James and E. Guth, *J. Chem. Phys.,* 1943, **11**, 455-481.
8. A. J. Chompff and J. A. Duiser, *J. Chem. Phys.* 1966, **45**, 1505-1514.
9. W. W. Graessley, *Macromolecules,* 1975, **8**, 186-190.
10. W. W. Graessley, *Polymeric liquids and networks : structure and properties*.
11. M. Rubinstein and R. H. Colby, *Polymer physics*; Oxford University Press: Oxford , New York, NY, 2003.
12. R.H. Ewoldt, M.T. Johnston and L.M. Caretta, Experimental Challenges of Shear Rheology: How to Avoid Bad Data. In: Spagnolie S. (eds) Complex Fluids in Biological Systems. Biological and Medical Physics, Biomedical Engineering; Springer: New York, NY, 2015.